

DEFORMATION AND FRACTURE BEHAVIOR DURING ANNEALING
OF RESIDUALLY STRESSED POLYCRYSTALLINE ALUMINUM OXIDE

by

Yenho Kuo Tree

Thesis submitted to the Faculty of the
Virginia Polytechnic Institute and State University
in partial fulfillment of the requirements for the degree of
MASTER OF SCIENCE
in
Materials Engineering

APPROVED:

D. P. H. Hasselman, Chairman

J. J. Brown, Jr.

M. R. Louthan, Jr.

April, 1982
Blacksburg, Virginia

ACKNOWLEDGEMENTS

The author would like to express his sincerest gratitude to Dr. D.P.H. Hasselman for his advice, guidance, patience and encouragement during the course of this study. Through many discussions with Dr. Hasselman and Anuradha Venkateswaran, the author gained valuable experience and understanding of this subject.

The author also wishes to thank Dr. J.J. Brown, Jr. and Dr. M.R. Louthan, Jr. for their advice and contributions to this thesis.

Financial support from the Army Research Office under Grant # DAAG 29-79-C-0193 is gratefully acknowledged. Also the help of Mr. T. Solberg with the microprobe analysis is appreciated. Lastly, the author wishes to thank his parents for their persistent and nagging encouragement that made completion of this work possible.

DEFORMATION AND FRACTURE BEHAVIOR DURING
ANNEALING OF RESIDUALLY STRESSED POLYCRYSTALLINE

ALUMINUM OXIDE

by

Yenho Kuo Tree

ABSTRACT

Three types of polycrystalline aluminum oxide, with varying amounts of impurities, were tempered and then annealed to study the behavior of residual stress relaxation. Results from microprobe analysis, thermal expansion analysis, annealed strength measurements, and scanning electron fractography clearly indicate stress relaxation at annealing temperatures occurred by elastic creep through crack nucleation and growth in regions under tensile stresses. From the scanning electron fractographs, it was found that intergranular glassy phase played an important role in the crack formation and propagation. At elevated temperature, viscous intergranular glassy phase behaved as an adhesive layer and when under tensile stresses caused de-adhesion of grain-boundaries or the formation of cracks. Fine-grained aluminas, with little or no glassy phase, exhibited both sub-critical and critical crack propagation. Since cracks decrease the load-carrying ability of the aluminas, it was concluded that by minimizing the glassy phase, porosity, grain size and residual stresses one can suppress crack formation.

TABLE OF CONTENTS

	PAGE
ACKNOWLEDGEMENTS.....	ii
ABSTRACT.....	iii
LIST OF FIGURES.....	v
LIST OF TABLES.....	vii
I. INTRODUCTION.....	1
II. EXPERIMENTAL.....	8
A. Materials.....	8
1. Materials Selection.....	8
2. Material Characterization.....	8
B. Experimental Procedure.....	10
1. Selection of Methods for Introduction of Continuum Residual Stresses.....	10
2. Tempering Experiments.....	11
3. Dilatometric Experiments.....	14
4. Strength Measurements.....	15
5. Residual Stress Fatigue.....	20
6. Scanning Electron Fractography.....	20
III. RESULTS AND DISCUSSION.....	21
A. Material Characterization.....	21
B. Dilatometric and Strength Degradation Results.....	30
1. AL-300 Alumina.....	30
2. ALSIMAG 614 Alumina.....	35
3. ALSIMAG 838 Alumina.....	38
4. Residual Stress Fatigue.....	38
C. Scanning Electron Fractography.....	42
D. General Discussion.....	52
IV. CONCLUSIONS.....	59
REFERENCES.....	60
APPENDIX.....	64
VITA.....	66
ABSTRACT	

LIST OF FIGURES

Figure		Page
1	Stress profiles for various methods of introducing continuum residual stresses.....	12
2	Apparatus for thermal tempering experiments.....	13
3	Apparatus for thermal expansion analysis.....	16
4	Three-point bending apparatus (separated).....	18
5	Four-point bending apparatus.....	19
6	Scanning electron fractograph of the as-received AL-300 alumina fractured at room temperature.....	22
7	Scanning electron fractograph of the as-received ALSIMAG 614 alumina fractured at room temperature.....	23
8	Scanning electron fractograph of the as-received ALSIMAG 838 alumina fractured at room temperature.....	24
9	Distribution of impurities in AL-300 alumina.....	26
10	Distribution of impurities in ALSIMAG 614 alumina.....	27
11	Distribution of impurities in ALSIMAG 838 alumina.....	28
12	Thermal expansion behavior of as-received AL-300 alumina.....	31
13	Thermal expansion behavior of residually stressed AL-300 alumina.....	32
14	Flexural strength of tempered AL-300 alumina after 25 min. anneal, as a function of annealing temperature.....	34
15	Thermal expansion behavior of tempered ALSIMAG 614 alumina.....	36
16	Flexural strength of tempered ALSIMAG 614 alumina after 25 min. anneal, as a function of annealing temperature.....	37
17	Thermal expansion behavior of tempered ALSIMAG 838 alumina.....	39

Figure	Page
18 Flexural strength of tempered ALSIMAG 838 alumina after 25 min. anneal, as a function of annealing temperature.....	40
19 Time-to-failure annealing treatments, under iso-thermal conditions, for the tempered ALSIMAG 838 alumina.....	41
20 SEM fractographs of tempered AL-300 alumina fractured at room temperature following annealing treatment at 900°C for 25 min. (a) near surface region (b) in specimen interior.....	43
21 Additional SEM fractographs of the tempered AL-300 alumina, followed by annealing treatment at 900°C for 25 min. (a) existence of glassy intergranular grain-boundary phase, and (b) finger-like crack growth indicating rapid grain-boundary de-adhesion at high temperatures.....	45
22 Intergranular crack propagation into the original compressive stress field, (a) as-received ALSIMAG 614 alumina fractured at room-temperature and (b) fracture behavior of tempered and then annealed ALSIMAG 614 alumina.....	46
23 Relative ratio of crack size (radius) to specimen radius.....	47
24 SEM fractographs of tempered ALSIMAG 614 alumina fractured at room temperature following annealing treatment at 950°C for 25 min. (a) near surface region and (b) in specimen interior.....	48
25 Critical crack propagation, during annealing, in tempered ALSIMAG 838 alumina resulting in a cup and cone fracture.....	50
26 SEM fractographs of the tempered ALSIMAG 838 alumina fractured during annealing treatment, (a) near surface region and (b) in specimen interior.....	51
27 Residual stress relaxation by crack growth (a) original stress distribution and (b) after annealing treatment.....	55

LIST OF TABLES

Table	Page
I Physical properties of the aluminas studied.....	9
II Grain and grain-boundary compositions of the aluminas.....	29

I. INTRODUCTION

In the past two decades, there has been an increasing demand for high temperature structural materials. Most of this demand has arisen from the accelerated growth of the aerospace, defense and energy related industries. Ceramic materials, because of their many advantageous properties, are well suited for high temperature structural applications. These properties include high melting point, high creep resistance, high abrasion resistance and excellent chemical stability. Some examples of the applications of ceramics are heat shields, rocket nozzles and nose-tips, turbine blades, cutting-tools, nuclear fuel pellets, and mechanical bearings.

Because of the highly brittle nature of ceramics, mechanical failure is often catastrophic. The failure originates at structural imperfections such as voids, impurities, microcracks and inclusions. The structural imperfections serve as crack nucleation sites and when critical load is applied, the crack will undergo unstable crack propagation. In order for ceramic components to be structurally useful, microstructure, impurities, surface flaws, etc., must be characterized intensively. By the use of sophisticated analytical techniques such as optical and electron microscopy, destructive and non-destructive testing techniques(1), structural imperfections may be minimized.

Another contributing factor to the mechanical behavior of ceramic components is the existence of residual stresses. Residual stresses are those stresses that would exist in a body if all external loads were removed. In a ductile material, the effects of residual stresses are

minimal, due to the plastic deformation mechanisms available. However, when a material is brittle, the tensile residual stresses may promote fatigue and reduce the fracture strength of the component. Similarly, compressive residual stresses may reduce the compressive load carrying ability of the component. Several terms have been used to refer to residual stresses such as: internal stresses, initial stresses, locked-in stresses, and thermal stresses(2). The usage of these terms depends on the circumstances in which the residual stresses were obtained. The most commonly used terms are "residual" or "internal" stresses. Residual stresses can be used advantageously as for surface compression strengthened window glass. In this case, the applied stress must first overcome the residual compression before the surface is brought into tension where failure can occur(3). However, residual stresses in precision optical glasses are a cause of optical stress birefringence. Therefore, residual stresses must be reduced by careful annealing procedures.

Residual stresses are classified into two basic categories, continuum residual stresses and micromechanical residual stresses. Continuum residual stresses refer to those stresses that exist over a distance of the order of the size of the component. The study of Cockbain(4) on silicon nitride indicates the magnitude of these residual stresses vary significantly within a component. Micromechanical residual stresses encompass those stresses that exist over a distance of the order of the grain size or the inclusion particle size.

Continuum residual stresses may be caused by processes such as non-

uniform drying and sintering(5,6), grinding and finishing operations(7,8), rapid heating and cooling rates(9), phase transformations(10), compositional non-uniformities(11), metal ceramic seals(12), and welded ceramic parts(13). Also, beneficial surface compression residual stresses may be achieved by the joining of two materials with non-equal coefficients of thermal expansion. Such examples would be coatings and laminates(14,15). In almost all cases the materials used for glazing would have a lower thermal expansion coefficient than the body. Micromechanical residual stresses in ceramic materials can arise due to mismatch in the coefficient of thermal expansion of the foreign inclusion particle and the host material(16) or the anisotropy of the individual grains(17). Also it has been noted that volume changes due to phase transformations may cause these stresses(18). Depending upon the material's thermal and mechanical history, micromechanical and continuum residual stresses may exist simultaneously. One must be able to determine the magnitude of these residual stresses because it will affect the load-carrying ability of the structural component. Other industry-related problems such as warping, deformation, chipping, cracking, etc., have been attributed to residual stresses in ceramic components(19).

For reliable design of structural ceramic components, there are two approaches in determining the magnitude of the existing residual stresses. The first approach is to use non-destructive testing (NDT) techniques to determine the residual stresses. However, due to the lack of simple NDT methods for measuring three-dimensional residual stresses,

this approach may not be feasible. The second approach is to subject the component to a thermal annealing treatment. By increasing the temperature, it may be possible to relax these stresses to a pre-selected minimum, whereby all of the components would have the same strength with minimum scatter. This would allow for more reliable engineering design using structural ceramic components. This approach, however, would require an understanding of the basic mechanisms of relaxation of the residual stresses.

Stressed solids can undergo time-dependent deformation known as creep. Extensive literature has discussed the mechanisms of creep such as dislocation glide and climb(20); diffusional processes such as Nabarro-Herring(21,22) and Coble(23) creep appear to be well understood.

For a residually stressed component without the existence of any external loads, the volume-averaged compressive and tensile residual stress field is equal to zero. Because of the coupled nature of residual stresses, stress relaxation in the compressive field will affect the stresses in the tensile field and also the reverse is true. Since the relaxation of stress encounters both compressive and tensile fields of large variations in magnitude, one would expect several mechanisms of residual stress relaxation.

Previous studies on residual stress relaxation in polycrystalline aluminum oxide were carried out by Krohn et al. (24). In the study by Krohn, the aluminum oxide selected was in the form of sintered circular rods with an average grain size of approximately 18 μm . Residual stresses were introduced into the specimens by quenching from 1450°C

into silicone oil at room temperature. The slotted-rod test may verify the existence of surface compression strengthening with the interior in tension. Stress relaxation was accomplished by annealing treatments at various temperatures for a duration of 25 minutes. Results of strength vs. annealing temperature showed that the strength sharply decreased from 70 ksi to 40 ksi between the temperature range of 775-800°C. By comparison of the creep rates and the activation energies of the mechanisms of creep known at that time, Krohn et al. attributed this stress relaxation to grain-boundary diffusion, ie., Coble creep.

Similar experimental results have been reached by Kirchner and Gruver(26). Two kinds of alumina were used in this experiment. One was sintered commercial grade 96% alumina and the other was hot pressed 99.7% alumina from Linde A powder. Samples were made in the form of cylindrical rods and residual stresses were introduced by similar quenching methods as those used by Krohn et al. Other than the differences in purity and grain size, the hot pressed alumina was not expected to have a glassy intergranular phase. Flexural strength was then measured at elevated temperatures. Results for the 96% alumina indicate that strength dropped rapidly from 750°C and leveled off at 25% of original tempered strength at 1000°C. Strength for the tempered hot pressed alumina at room temperature was significantly higher than that of the 96% alumina. At elevated temperatures similar strength losses occurred for the hot pressed alumina. However, the temperature range for this loss shifted to approximately 1000°C to 1300°C for the hot pressed alumina as compared to 750 to 1000°C for the 96% alumina.

Kirchner and Gruver offered no explanation for this difference.

Differences in the stress relaxation temperature range may be due to the existence of the glassy intergranular phase of the 96% alumina(27).

The study by Kirchner and Gruver also included time dependent experiments. Specimens of the 96% alumina were quenched and then heated to the "stress relaxation region" at 850 or 900°C for a period of four hours to see if stress relaxation was time dependent. No changes in the strengths were detected and therefore stresses were not significantly relieved in four hours.

Considering all the creep mechanisms known at that time, such as dislocation, diffusional or viscous creep, neither process can provide the magnitude of creep required for major stress relaxation at that temperature and stress level. Even the diffusional creep mechanism, which is expected to be dominant at this temperature and stress level, would require a temperature greater than $0.5 T_m$ (greater than 1150°C) to have a significant contribution to stress relaxation.

However, it is now believed that creep by crack growth proposed by Hasselman(28) some years ago may be an important mechanism in this stress relaxation process. Hasselman proposed that for a material with randomly oriented microcracks subjected to triaxial tensile stresses, the material may creep at low temperatures by growth of these cracks. A more recent paper by Hasselman and Venkateswaran(29) revealed that crack growth can contribute to time-dependent changes in elastic properties, which in this case could lead to residual stress relaxation.

From the results of Krohn, and Kirchner and Gruver, annealing

treatments on residually stressed polycrystalline aluminum oxide showed unexpected strength losses at temperatures near 750°. For both cases the strength dropped well below the as-received strength. If this stress relaxation process occurs by crack formation and growth, then stress relaxation by annealing treatments may be undesirable. This is because the presence of cracks is not expected to enhance the load bearing ability of the component. Also, if residual stresses were introduced in a structural component for strengthening purposes, it can not be used beyond 775°C. It is the objective of this study to develop increased understanding of the behavior of residually stressed ceramics subjected to annealing treatments, with special emphasis on the role, if any, of cracks during the stress relaxation.

II. EXPERIMENTAL

A. Materials

1. Materials Selections

The aluminum oxide chosen for this thesis contains varying amounts of impurities expected to exist as glassy phases. Aluminum oxide was chosen because many previous residual stress studies have been focused on it and many basic properties of this material are well understood. Three types of alumina were obtained from commercial sources: AL-300^{*}, ALSIMAG 614 and 838^{**}. The specimens were in the form of long solid circular cylinders approximately 0.504 cms in diameter. These rods were then cut into 2.2 cm sections with a low-speed, circular diamond saw. Their physical properties as listed by the manufacturers are given in Table I.

2. Material Characterization

The composition and distribution of the chemical constituents in each alumina was examined by electron microprobe analysis. The aluminas were mounted in liquid plastic molds and then polished with 1 μ m and 0.3 μ m diamond paste respectively. The samples were coated with approximately 200 $\overset{\circ}{\text{A}}$ of carbon and x-ray scanning photographs were taken. These photographs give an indication of the distribution of a particular element. Silicon (Si), calcium (Ca), magnesium (Mg) and aluminum (Al)

* AL-300, Western Gold and Platinum Co., Belmont CA, USA.

** ALSIMAG 614 and 838, American Lava Corp., 3M Company, Chattanooga TN, USA.

TABLE I : PHYSICAL PROPERTIES OF THE ALUMINAS STUDIED

	<u>AL-300 (30)</u>	<u>ALSIMAG 614 (31)</u>	<u>ALSIMAG 838 (31)</u>
Modulus of Elasticity (GPa)	358	324	344
Shear Modulus (GPa)	145	131	145
Poisson's Ratio	0.24	0.22	0.22
Flexural Strength (MPa)	238	317	447
Thermal Expansion ($\times 10^{-6}/C^{\circ}$)	7.9	7.9	7.7
Purity Al_2O_3 (%)	99.3	96.0	99.5

were the major elements detected. Microprobe compositional analyses were also done on the alumina body and the grain-boundaries. The microprobe used was an ARL-SEMQ operating at 15 Kev.

B. Experimental Procedure

1. Selection of Methods for Introduction of Continuum Residual Stresses

Continuum residual stresses can be introduced in ceramics by cladding (32,33), ion exchange(34,35), or thermal tempering(36,37). In the cladding process, a material is coated with a layer of material of a lower coefficient of thermal expansion at a relatively high temperature. Upon cooling, the surface layer contracts less; therefore, it is in a state of compression on reaching thermal equilibrium. This process, however, would create unnecessary complications in both processing and analysis due to the two different materials.

Ion exchange strengthening is accomplished by the exchange of small monovalent cations for larger ones at the specimen surface. The larger cations will crowd the surface layers to produce a surface compressive stress. High residual stresses are possible at the extreme surface layers by this method. However, this method cannot be used for this study, because at annealing temperatures stress relaxation will occur by diffusion of the larger ions.

In thermal tempering processes, the ceramic is heated to its softening temperature and quenched into a cooler medium. Upon quenching, the specimen's exterior cools rapidly while the interior is

still hot and viscoelastic. The material is essentially stress free at this point. However, when the interior cools further, the contraction of the interior is restrained by the rigid surface layers, resulting in a residual stress field once thermal equilibrium is achieved.

A critical requirement for the annealing studies is that the residual stresses introduced in the specimens must be of known magnitude and approximate distribution. As can be seen in Figure 1, the stress profile of the quench specimen gives the widest range of stress levels. Therefore, by quenching the aluminum oxide, stress relaxation can be studied over a wide range of stress levels. Due to the geometry of the cylindrical specimens, the stress profile is expected to be radially symmetric. Buessem and Gruver(38) have made calculations of the magnitude and distribution of the residual stresses in quenched 96% alumina. Since the introduction of residual stress by quenching offers the widest range of stress levels, whose magnitude and distribution are well known, quenching methods will be chosen for this thesis.

2. Tempering Experiments

For thermal tempering, the process involves heating the three types of alumina to sufficiently high temperature and quenching them into a suitable medium. An induction furnace, shown in Figure 2, was used for this purpose. The induction heating unit consisted of a cylindrical graphite susceptor with five 0.8 cm diameter and 9 cm deep holes drilled equidistant from the center and protected by a fused quartz tube on the exterior. The induction coil was placed on the outside of the quartz

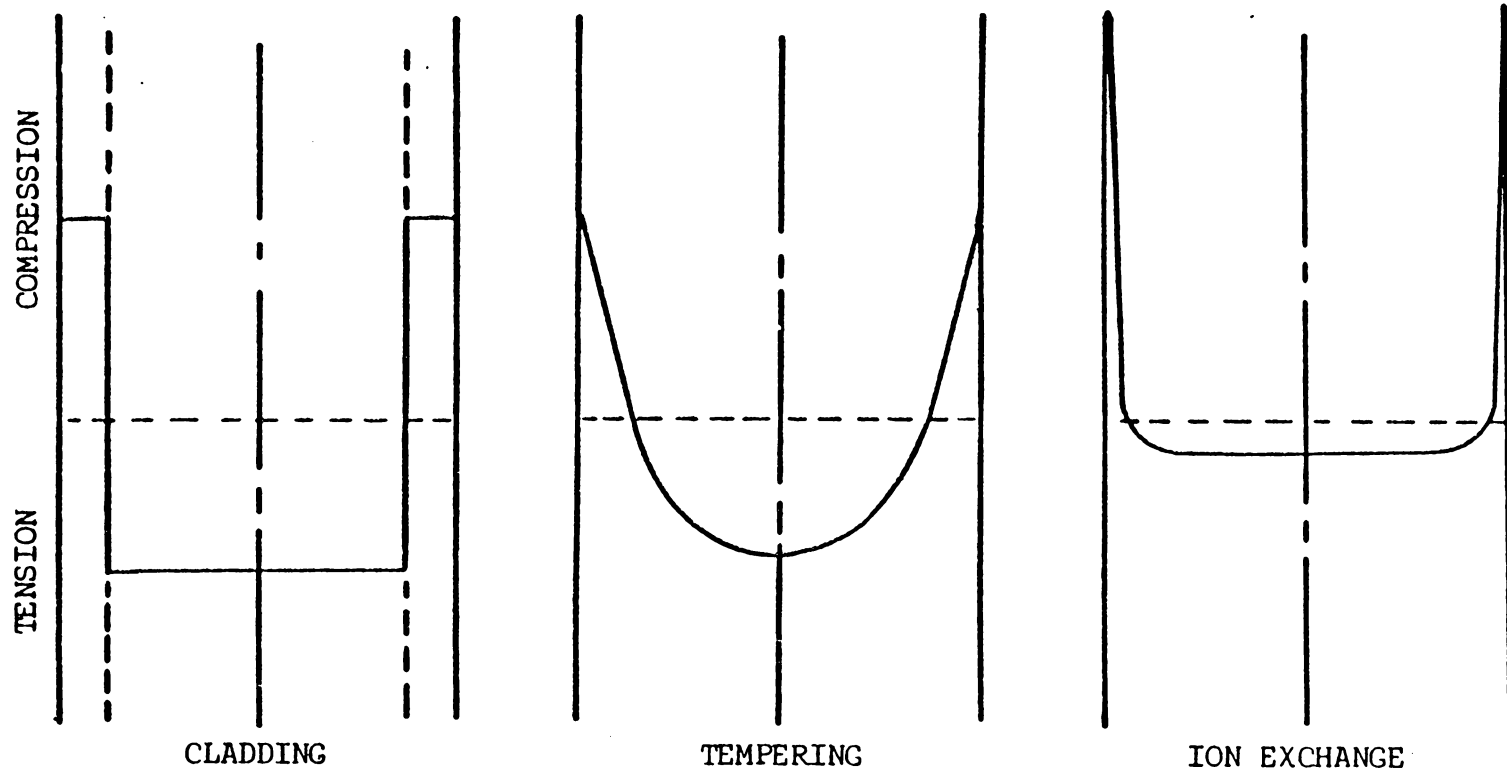


Fig. 1. Stress profiles for various methods of introducing continuum residual stresses.

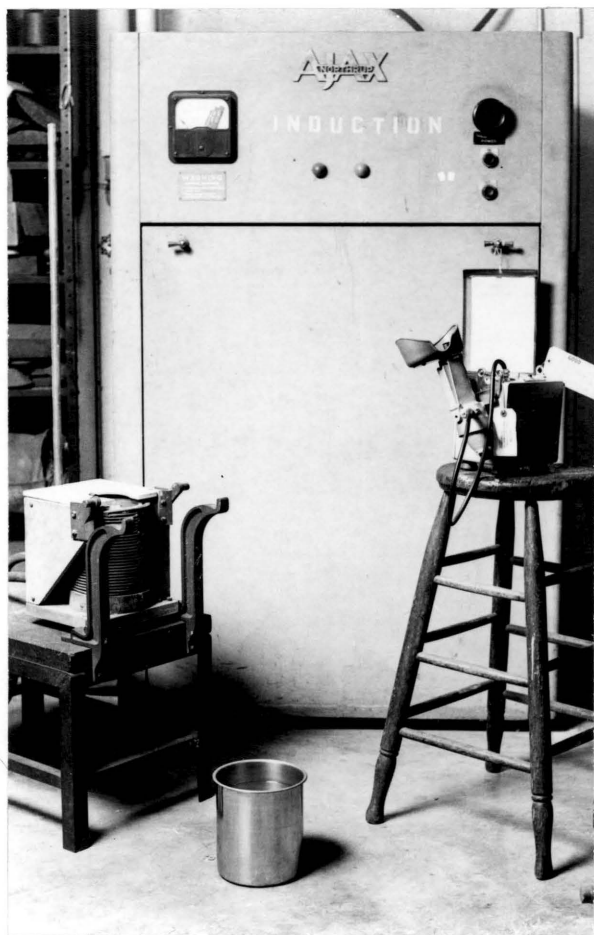


Figure 2. Apparatus for thermal tempering treatments.

tube. Each alumina rod was first cut into sections of approximately 2.2 cms and then placed into the holes within the graphite susceptor for heating.

The softening temperature for the AL-300, ALSIMAG 614 and ALSIMAG 838 are 1450, 1550, and 1600°C respectively. A heating rate of approximately 80°C per minute was used, reaching the softening temperature in 20 minutes. Specimens were held at this temperature for six minutes to reach thermal equilibrium(39) and then quenched into a 100 cts. silicone oil* bath at room temperature. Decomposition products of carbon and excess oil were bonded to the specimen surface. Therefore, ultrasonic cleaning with acetone was used.

The temperature of the induction heater was monitored using an optical pyrometer. An accuracy of $\pm 10^{\circ}\text{C}$ can be achieved with a calibrated pyrometer.

3. Dilatometric Experiments

Stress relaxation can occur in ceramics by several well known creep mechanisms. A distinction between creep mechanisms could be made by studying stress relaxation during thermal expansion measurements. If crack growth is a significant mechanism in low temperature stress relaxation, then permanent dimensional changes of the specimen in addition to normal thermal expansion should be detected during heating. As indicated by Kirby(40), factors such as residual stresses(41,42),

*Silicone Oil, Dow Corning, Type 200, 100 cts.

formation of cracks and point defects(43), chemical composition (above 1%), and quantity and size of phases(44,45) can have a significant effect on the thermal expansion. Since stress relaxation by crack growth is expected to add only a few μm to the total expansion, sensitive dilatometers can measure the thermal expansion required. This experiment can lead to great insight into the behavior of residually stressed alumina during annealing.

The dilatometer used for this study was a Dupont thermal mechanical analyzer (TMA). The apparatus for thermal expansion is shown in Figure 3. Samples of each alumina were tested in the quartz sample holder at a heating and cooling rate of 10°C per minute* in order to avoid excess thermal stresses. At this heating rate, the thermal stresses were calculated to be in the order of 140 KPa (20 psi) which are too low to have a significant effect on the relaxation of the residual stresses.

Many specimens of each type of alumina in both as-received and tempered rods were tested in order to test repeatability. These runs were calibrated with a high purity Lucalox**. The thermal expansion of the Lucalox was compared with that of a handbook value(46) and a calibration curve was established.

4. Strength Measurements

A number of tempered specimens from AL-300, ALSIMAG 614 and 838

* See Appendix I for stress calculations for $10^{\circ}\text{C}/\text{min}$.

** Lucalox, General Electric, Lighting Business Group, Cleveland Ohio, USA.

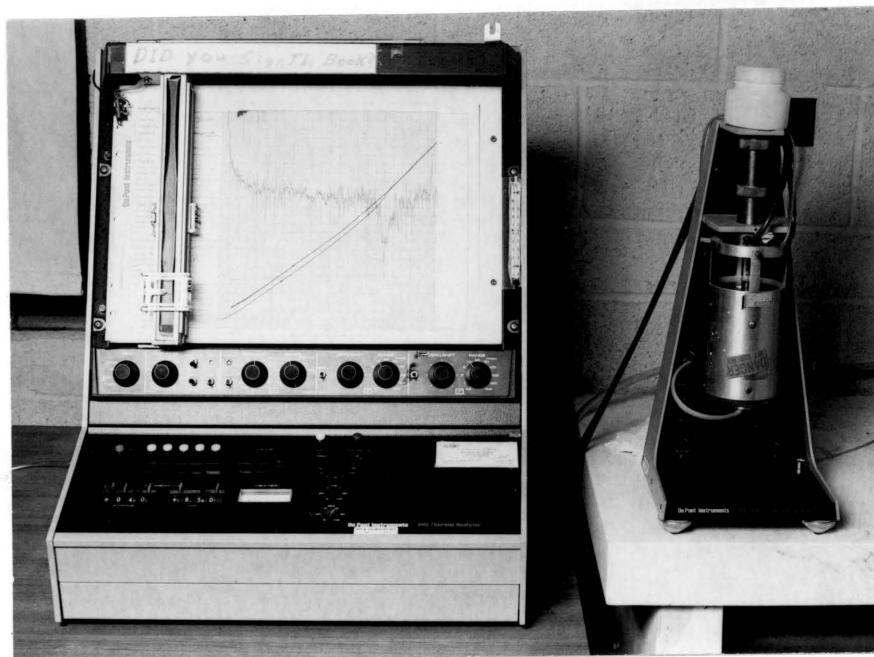


Figure 3. Apparatus for thermal expansion analysis.

were annealed using the Dupont TMA as a controlled furnace. The annealing temperatures ranged from 600°C up to 1200°C. Heating rates of 10°C/min were used to bring the specimen up to the specified temperature and the specimen was held at that temperature for 25 minutes to obtain thermal equilibrium. Specimens were then cooled at the same rate of 10°C/min.

Following the annealing treatments, the specimens were tested for strength degradation. The majority of the strength testing was done using a three-point bending apparatus with an outer span of 1.27 cms. This apparatus is shown in Figure 4. The load was applied by a compressive Instron machine at a crosshead speed of 0.5 cm/min. Due to the length limitation of the TMA of 2.54 cms, the maximum size of the annealed specimens was only 2.2 cms. Therefore, only small spans for three-point bending can be used. This would result in a low span-to-diameter ratio causing overestimates of the tensile failure stresses, so that relative rather than absolute strength values should be used for evaluation of the data. However, for purposes of comparison, long span four-point bending apparatus, shown in Figure 5, were used for comparison of as-received AL-300 aluminas. Outer and inner spans are 4.93 and 1.65 cms respectively. The same crosshead speeds of 0.5 cm/min were used for both three and four point bend tests. The strengths for both three- and four-point bending was calculated from:

$$S = \frac{16 L a}{3.14 D^3}$$

where L = load, D = specimen diameter, a (three-point) = half-span length, a (four-point) = moment arm length between outer and inner

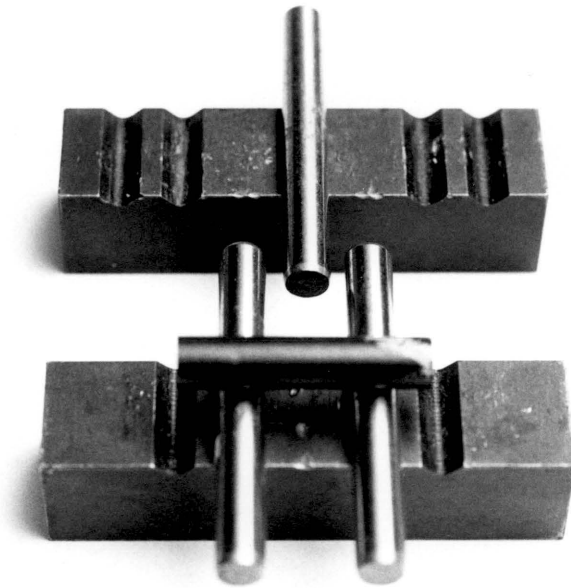


Figure 4. Three-point bending apparatus (separated).

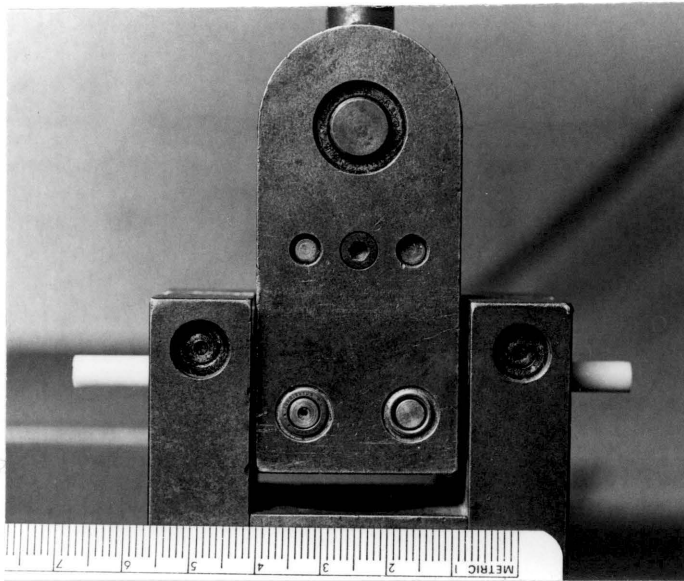
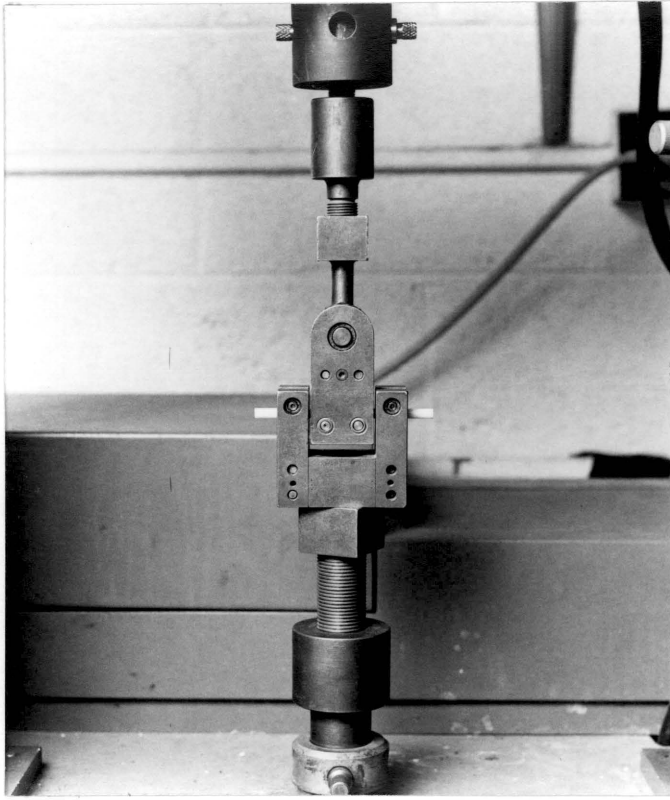


Figure 5. Four-point bending apparatus.

supports.

5. Residual Stress Fatigue

Tempered ALSIMAG 838 aluminas were held at a specified temperature for a period of 24 hours, over a temperature range from 600 to 900°C. The TMA was used to provide the iso-thermal conditions required for this time-dependent experiment. A timer was connected to the control unit of the TMA so that any changes in thermal expansion during the iso-thermal period would stop the timer. This method provides precise time-to-failure data for residual stress fatigue.

6. Scanning Electron Fractography

Fracture surfaces of the three types of alumina used, in both as-received and tempered conditions, were examined by scanning electron microscopy.* The specimens were mounted on a holder and coated with ^o200Å of carbon. The image was produced using secondary electrons, under an operating condition of 20 Kev.

* ARM-900, American Metals Research, Bedford MA, USA.

III. RESULTS AND DISCUSSION

A. Material Characterization

Room temperature scanning electron fractographs of the as-received aluminas are shown in Figures 6 through 8. The scanning electron fractograph of the AL-300 alumina indicates the average grain size was near 25 μm with an occasional grain size as large as 40 μm . Extensive residual pore-phase existed in the material with the majority of them located at grain-boundaries and triple points. Sections of the fracture surfaces appeared smooth and small cleavage steps were present indicating transgranular fracture. Other sections of the fracture surfaces appeared rough with smooth grain facets indicating intergranular fracture.

For the ALSIMAG 614 alumina, average grain size was near 5 μm . Some residual pore-phase existed at triple points only. This may be due to the Mg added for densification purposes. Similar to the AL-300 alumina, fracture surfaces of ALSIMAG 614 alumina were dominated by both intergranular and transgranular fractures. However, for the ALSIMAG 838 alumina, the majority of the fracture surfaces were intergranular fractures. The average grain size was near 4 μm with few dispersed pores.

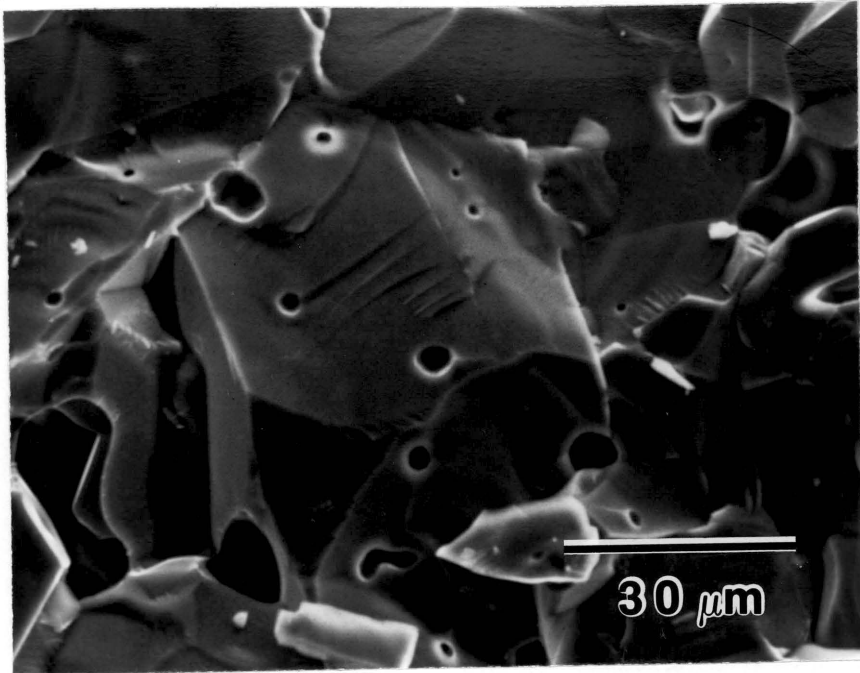


Figure 6. Scanning electron fractograph of the as-received Al-300 alumina fractured at room temperature.

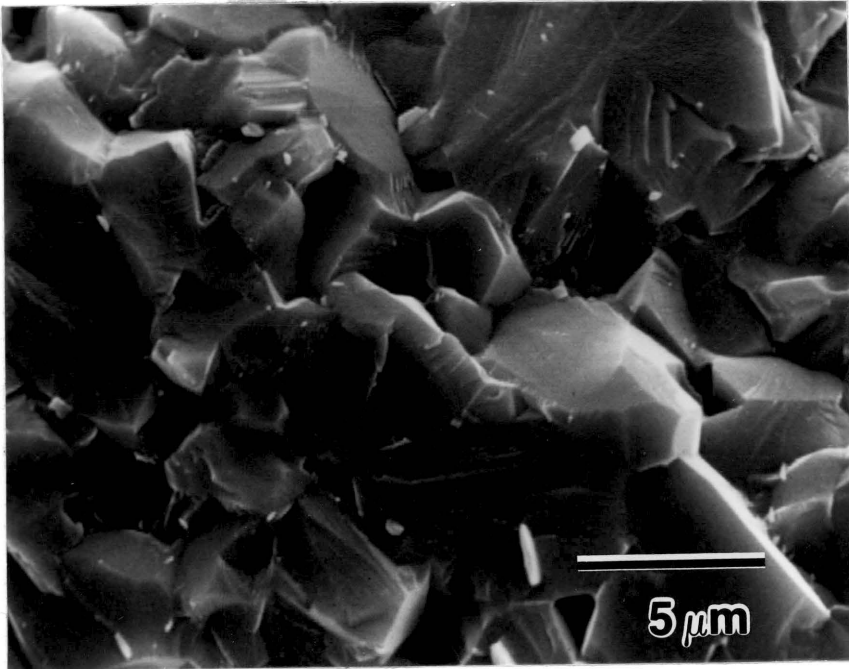


Figure 7. Scanning electron fractograph of the as-received ALSIMAG 614 alumina fractured at room temperature.

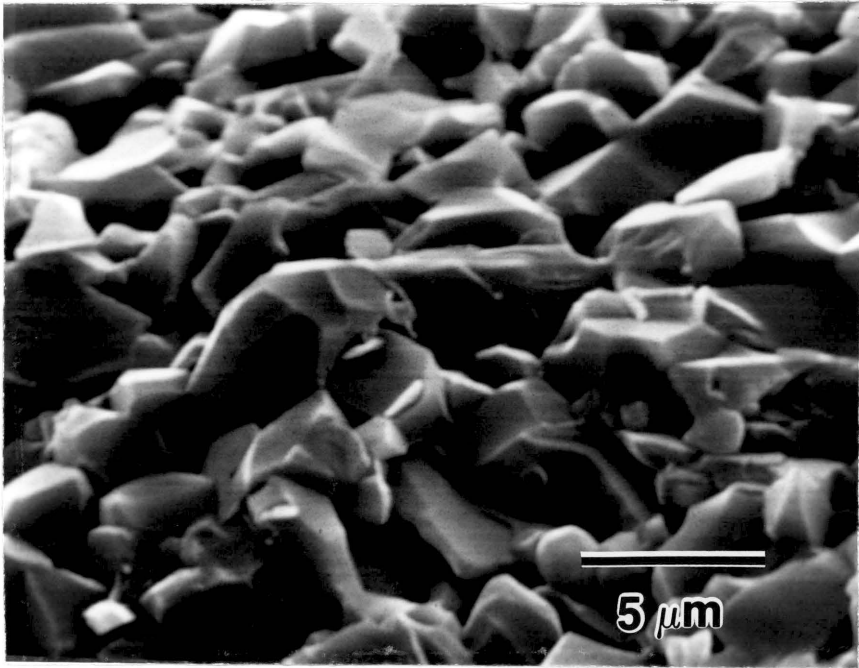


Figure 8. Scanning electron fractograph of the as-received ALSIMAG 838 alumina fractured at room temperature.

Microprobe element distribution maps of the AL-300, ALSIMAG 614 and 838 aluminas are shown in Figures 9, 10, and 11 respectively. Clearly for the AL-300 alumina shown in Figure 9, Al was found at the grains and the Ca and Si impurities existed at the grain-boundaries. Other impurities such as Mg and Fe, not shown, also occupied the same sites as Ca and Si. This suggests that these impurities exist in the form of residual calcium-alumino-silicate glass phase at the grain-boundaries. In Figure 10, SEM photomicrograph of the ALSIMAG 614 polished section shows the configuration and locations of the grain-boundary. As can be seen from the three element distribution maps, the impurities occupy the grain-boundary sites. Although in a much lesser quantity due to the ALSIMAG 838 purity, Figure 11 reveals the same results.

From the microprobe compositional analysis, results of the grain and grain-boundary composition are presented in Table II. Because of the unknown analytical depth of the microprobe and the thickness of the grain-boundaries, these results should be used for qualitative comparisons only.

Differences in the grain and grain-boundary composition of the AL-300 alumina are of the largest magnitude of all three aluminas. At the grains, all three aluminas contain high purity Al. At AL-300 alumina grain-boundaries, the composition broke down evenly between Al, Ca, and Si, giving further evidence of a calcium-alumino-silicate glass phase. However, at the ALSIMAG 614 grain-boundaries, the Ca content was reduced leaving alumino-silicate glass phase. In ALSIMAG 838 alumina grain-boundaries, Ca and Si both exist at low concentrations, while Mg

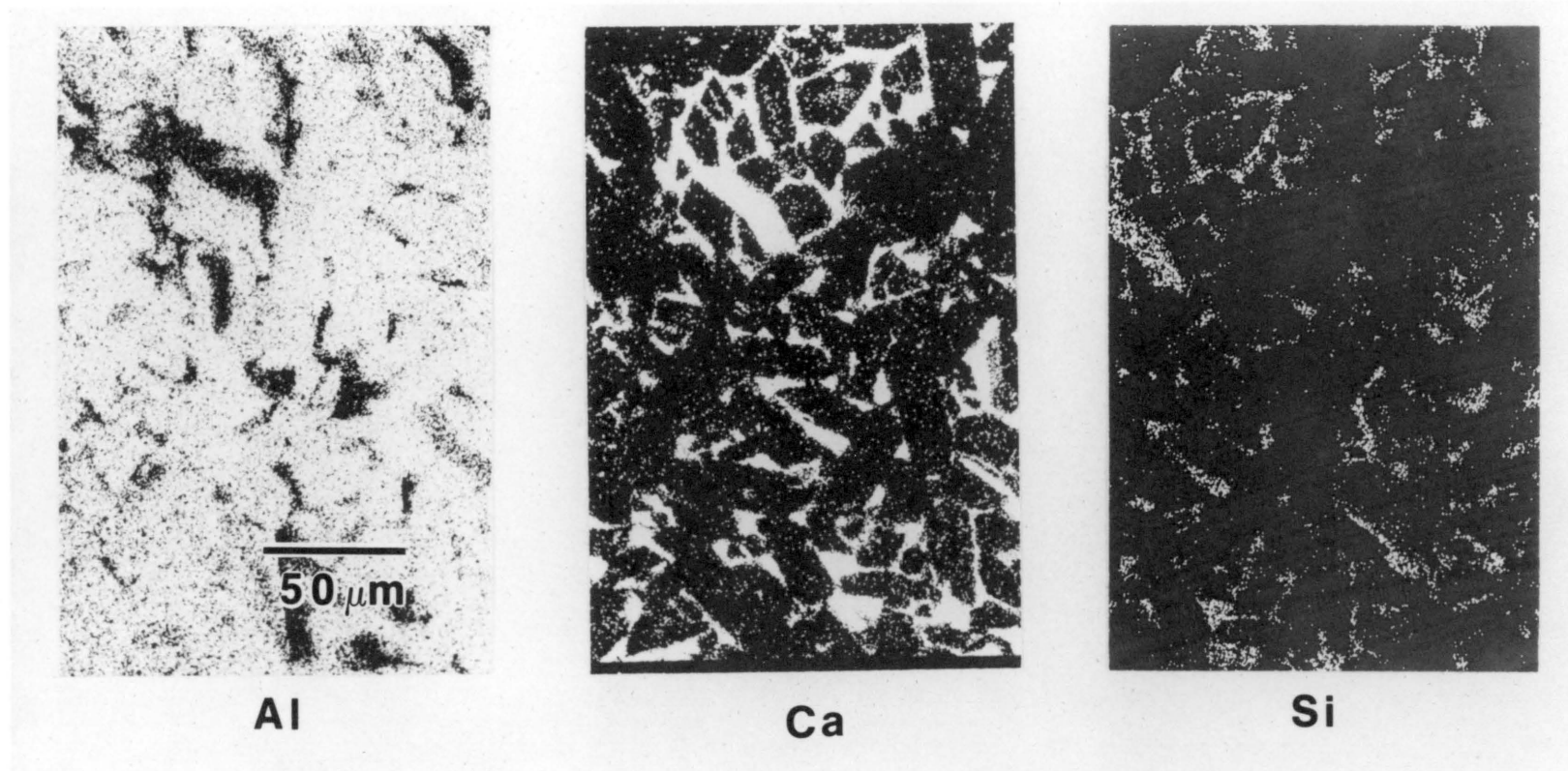


Figure 9. Distribution of impurities in Al-300 alumina.

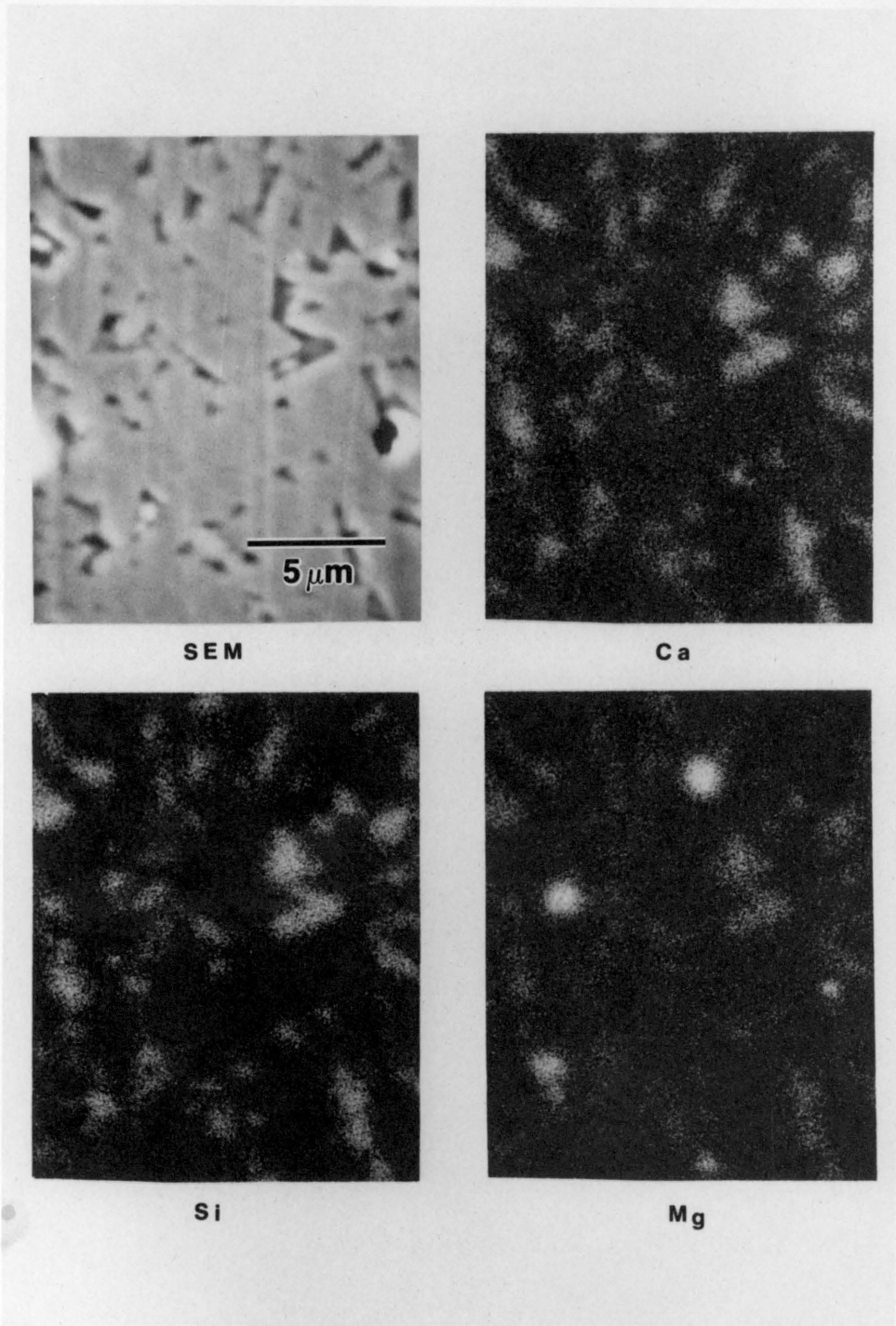
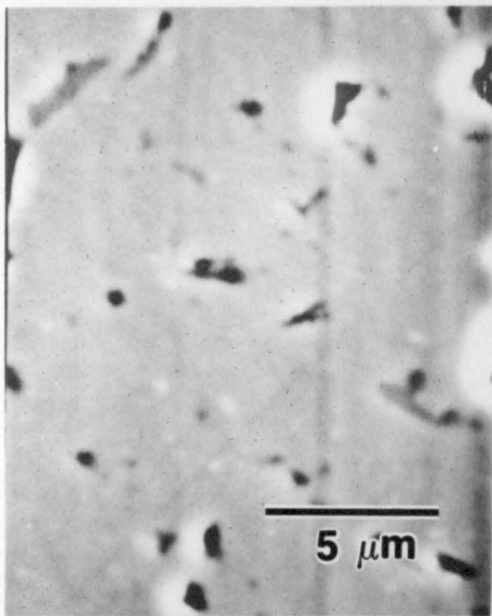


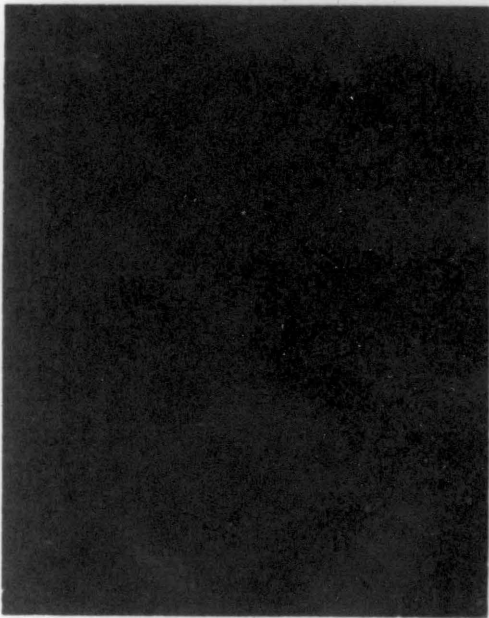
Figure 10. Distribution of impurities in ALSIMAG 614 alumina.



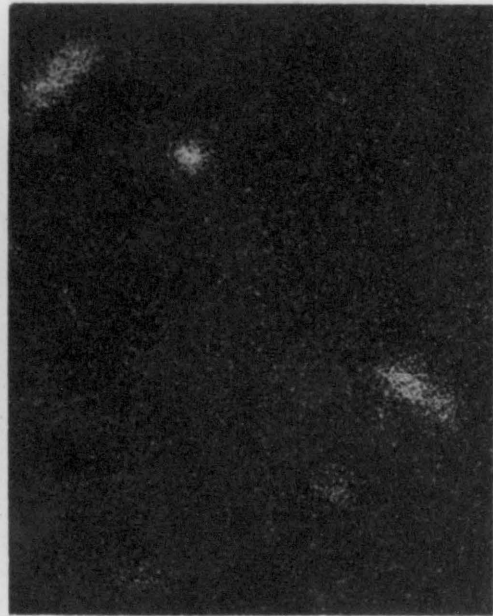
SEM



Ca



Si



Mg

Figure 11. Distribution of impurities in ALSIMAG 838 alumina.

TABLE II: GRAIN AND GRAIN-BOUNDARY COMPOSITION OF THE ALUMINAS*

(element)	AL-300		ALSIMAG 614		ALSIMAG 838	
	GRAIN	GRAIN- BOUNDARY	GRAIN	GRAIN- BOUNDARY	GRAIN	GRAIN- BOUNDARY
Al ₂ O ₃	99.79	32.26	99.77	77.66	99.76	92.69
CaO	0.00	27.61	0.01	0.97	0.00	1.34
SiO ₂	0.00	37.52	0.09	18.94	0.00	1.48
MgO	0.04	0.69	0.05	1.08	0.04	3.37
FeO	0.03	0.80	0.03	0.07	0.02	0.07
Na ₂ O	0.01	0.27	0.01	0.05	0.00	0.84

* All data are given in weight %.

is the dominating impurity. The results of the microprobe compositional analysis are in good agreement with the element distribution maps. Both results indicate the impurities existed at the grain-boundaries and triple points as residual glassy phase.

B. Dilatometric and Strength Degradation Results

1. AL-300 Alumina

Figure 12 shows the thermal expansion data for an as-received and annealed specimen. The dilatometric curve shows the monotonic increase in specimen dimension with increasing temperature. The thermal expansion data lie slightly below the recommended data for a high-purity, dense and fine-grained alumina(29). This is because the presence of glassy-phase permits grain-boundary separation due to thermal expansion anisotropy of the individual grains. However, the result is in good agreement with literature data.

In contrast to the monotonic increases of the as-received aluminas, the thermal expansion for the tempered AL-300 alumina shown in Figure 13 clearly shows discontinuous behavior at the higher temperature ranges. At temperature range between 875 to 950°C, the rate of thermal expansion increases rapidly and then tapers off to the original expansion rate. Below and above this temperature range, thermal expansion is similar to the as-received alumina. This discontinuous behavior does not exist during cooling. Thus the mechanism responsible for the discontinuous behavior appears to be irreversible and leads to permanent increase in length on return to room temperature. A permanent deformation of

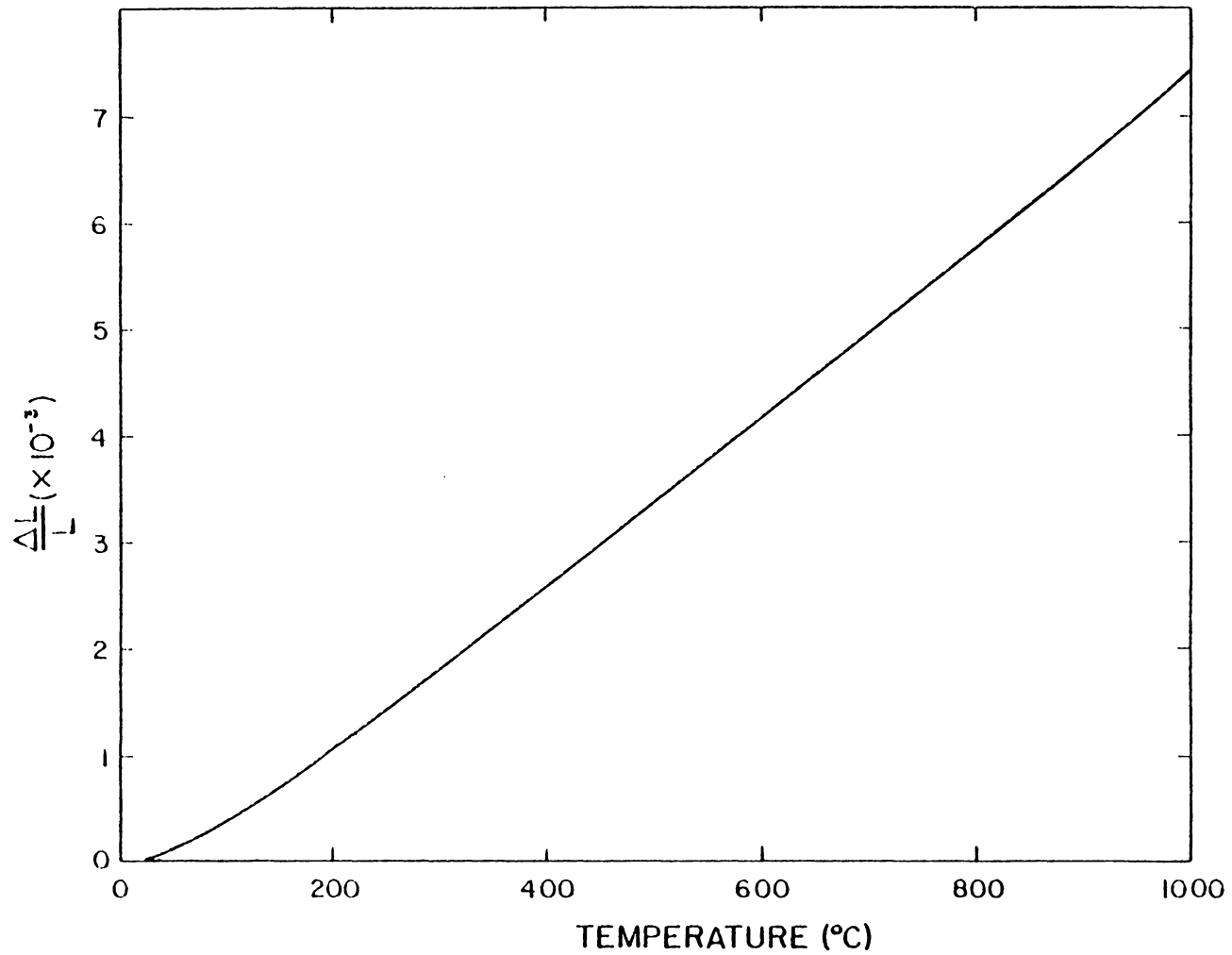


Figure 12. Thermal expansion behavior of as-received Al-300 alumina.

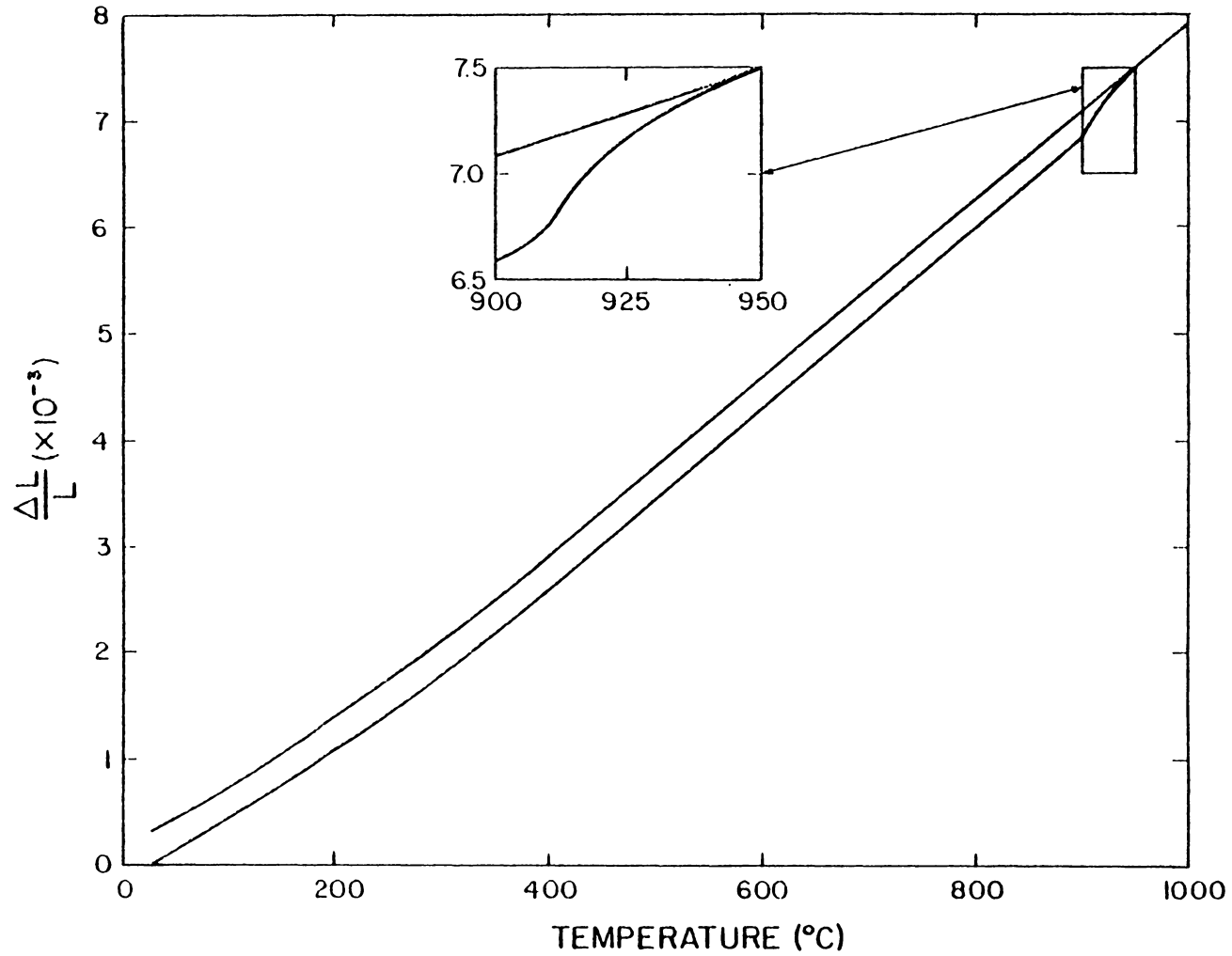


Figure 13. Thermal expansion behavior of residually stressed Al-300 alumina.

approximately 7 μm was measured for a specimen of 2.2 cm.

It was further observed that tempered AL-300 aluminas annealed for 25 minutes between 800°C to 1000°C temperature range showed a large decrease in fracture stress, as shown in Figure 14. Average room temperature three-point flexural strength of tempered alumina was 958 MPa. A 75% increase from the strength of the as-received alumina was obtained. With increasing annealing temperature from 800°C to 1000°C the strength gradually decreased from 825 MPa to 565 MPa, which is 20 MPa higher than the average of the as-received strength. A total of four specimens were tested at each temperature. No stress relaxation was observed for annealing temperatures less than 800°C.

Although three-point tests overstate the strength results, a comparison of the as-received AL-300 alumina with four-point tests showed a fairly consistent increase. The average flexural strength of ten specimens from the three-point tests was 545 MPa, compared to 238 MPa for the four-point tests.

Apparently, the discontinuous behavior in thermal expansion shown in Figure 13 is associated with the relaxation of residual stresses, because both phenomena occurred in the same temperature range. There were no measurable changes in the specimen diameter, so there was a net volume increase after the annealing treatment. Tentatively, by considering all the stress relaxation processes available at this temperature and stress level, the results indicate the formation of cavities or cracks may be the most likely mechanism.

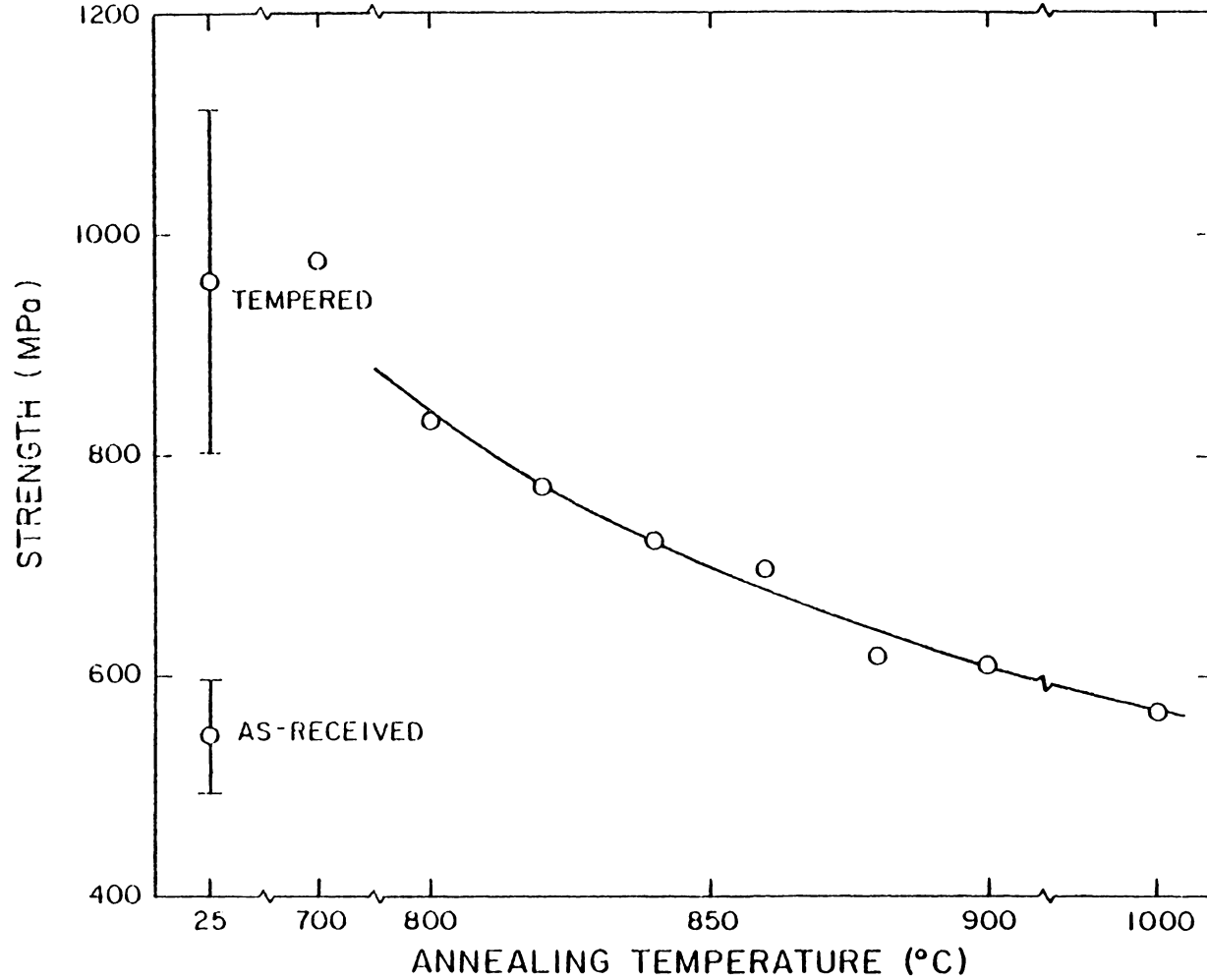


Figure 14. Flexural strength of tempered Al-300 alumina after 25 min. anneal, as a function of annealing temperature.

2. ALSIMAG 614 Alumina

Thermal expansion for the as-received and annealed ALSIMAG 614 alumina occurred in a monotonic fashion. Similar discontinuous dilatometric behavior, shown in Figure 15, was observed for ALSIMAG 614 alumina. Discontinuous behavior occurred between the temperature range of 850 to 1050°C. The rate of increase in thermal expansion is irregular in this temperature range. The permanent dimensional increase, after cooling to room temperature, was about 15 μm for a 2.2 cm specimen.

Majority of the residual stresses were relieved by the first rapid increase in thermal expansion rate at 850°C. This can be substantiated by the results of strength measurements as a function of annealing temperature, shown in Figure 16. Average of ten tempered specimens exhibited a flexural strength of 1340 MPa with a standard deviation of 76 MPa. The tempering treatment increased the as-received strength by 670 MPa. Compared to the AL-300 alumina, tempered ALSIMAG 614 alumina achieved a 25% larger increase in strength. At an annealing temperature of 850°C, the tempered specimen strength dropped from 1190 MPa at 825°C to 312 MPa at 850°C. Beyond the annealing temperature of 850°C, the strength remained constant.

It is important to notice that both the sharp decrease in strength and the discontinuity in thermal expansion occurred at 850°C. Also, the strength of the tempered ALSIMAG 614 alumina is lower than the as-received strength after the 850°C annealing treatment. From these observations, one may tentatively contribute the cause of strength loss

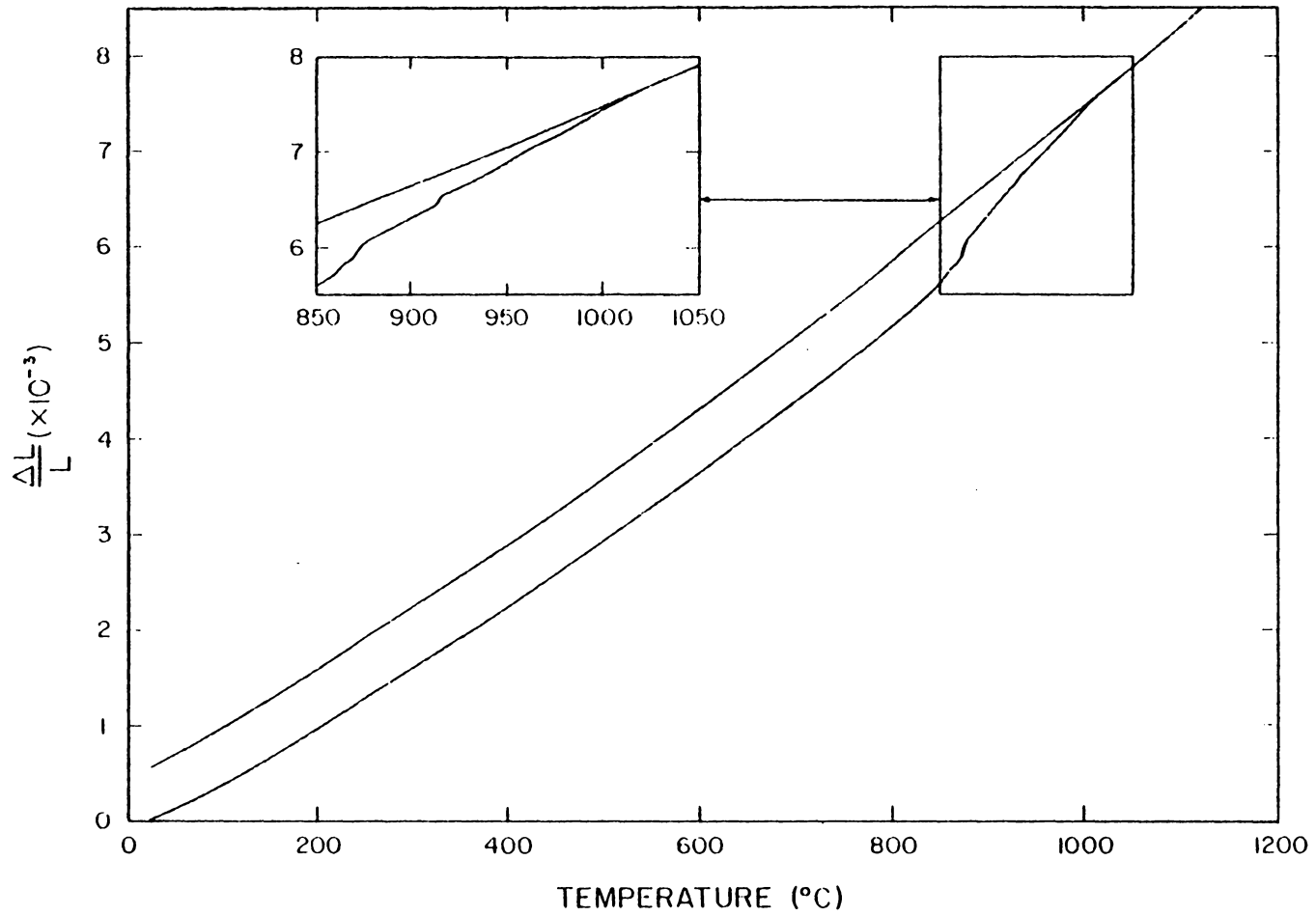


Figure 15. Thermal expansion behavior of tempered ALSIMAG 614 alumina.

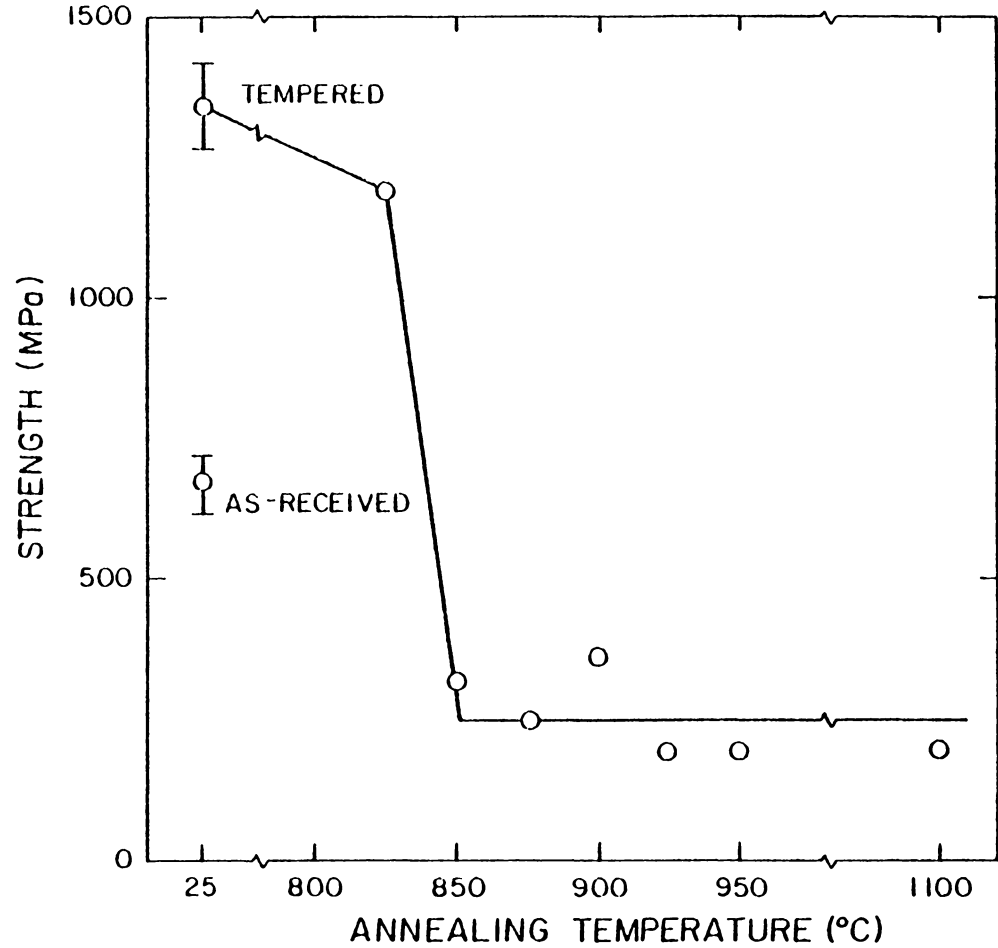


Figure 16. Flexural strength of tempered ALSIMAG 614 alumina after 25 min. anneal, as a function of annealing temperature.

to cavitation or crack formation.

3. ALSIMAG 838 Alumina

Dilatometric curve for the ALSIMAG 838 alumina is shown in Figure 17. In contrast to the other aluminas with a glassy grain-boundary phase, this high purity, fine grained alumina exhibited sudden thermal expansion increases, or "pop-in" affect. Majority of the "pop-in" occurred between 700 to 800°C. After the dilatometric measurements, some specimens fractured into two sections in a cup and cone fashion. SEM photographs of this fracture will be presented in a later section.

Specimens that did not segregate into two sections during annealing treatments retained little or no strength. This is shown in Figure 18. For the 1600°C tempering treatment, strength was increased from 640 MPa in the as-received condition to 1400 MPa. At annealing temperatures above 800°C, strength dropped to only a few MPa.

Similar observations were made with samples tempered at 1550°C. Strength increases by tempering at this temperature were less than the tempered strength at 1600°C. For specimens that were tempered at 1550°C, annealing results indicate increases in scatter at different annealing temperatures.

4. Residual Stress Fatigue

The results of the fatigue studies are presented in Figure 19. At 600 and 700°C only one specimen of the tempered ALSIMAG 838 alumina failed during the 24 hour period. Additional specimens failed during

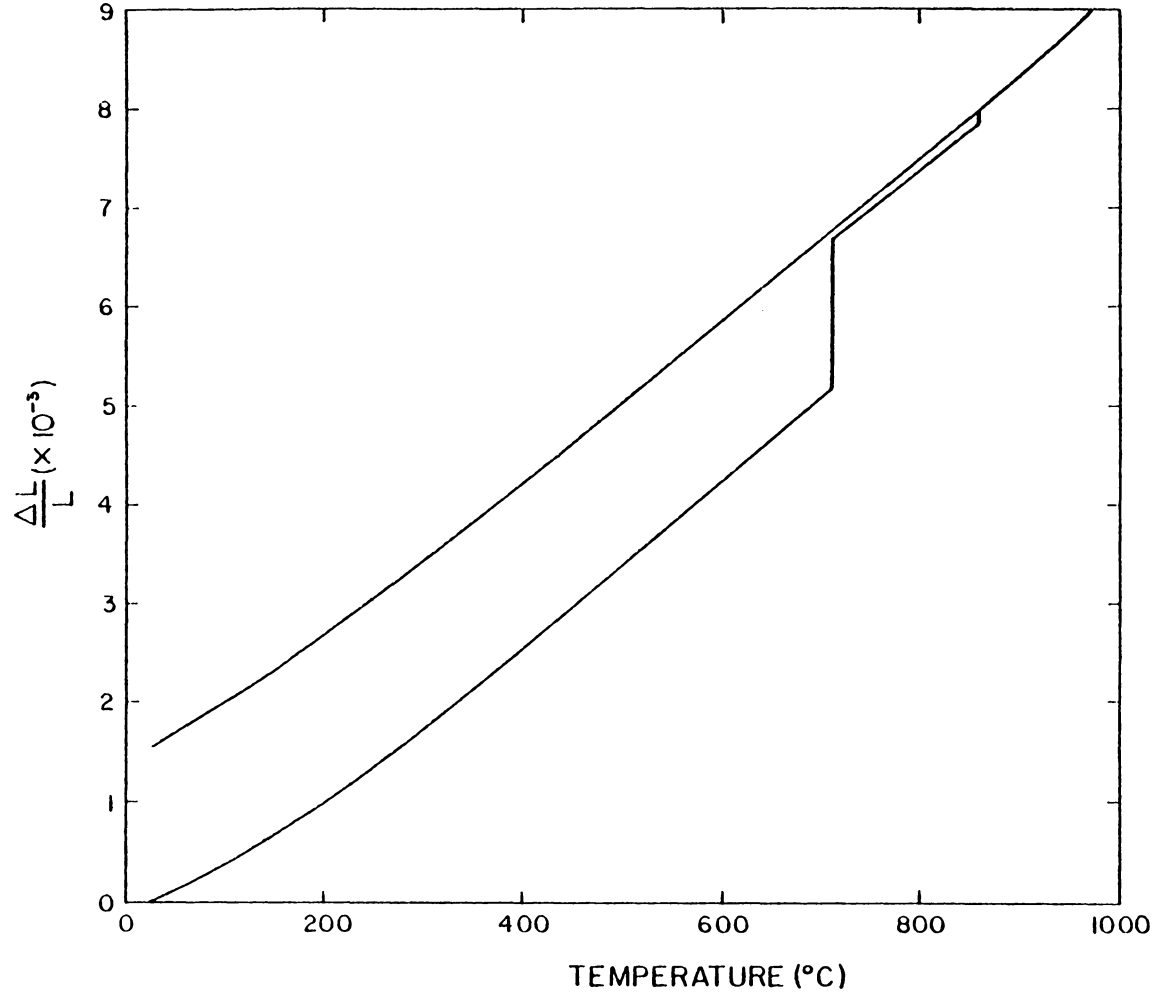


Figure 17. Thermal expansion behavior of tempered ALSIMAG 838 alumina.

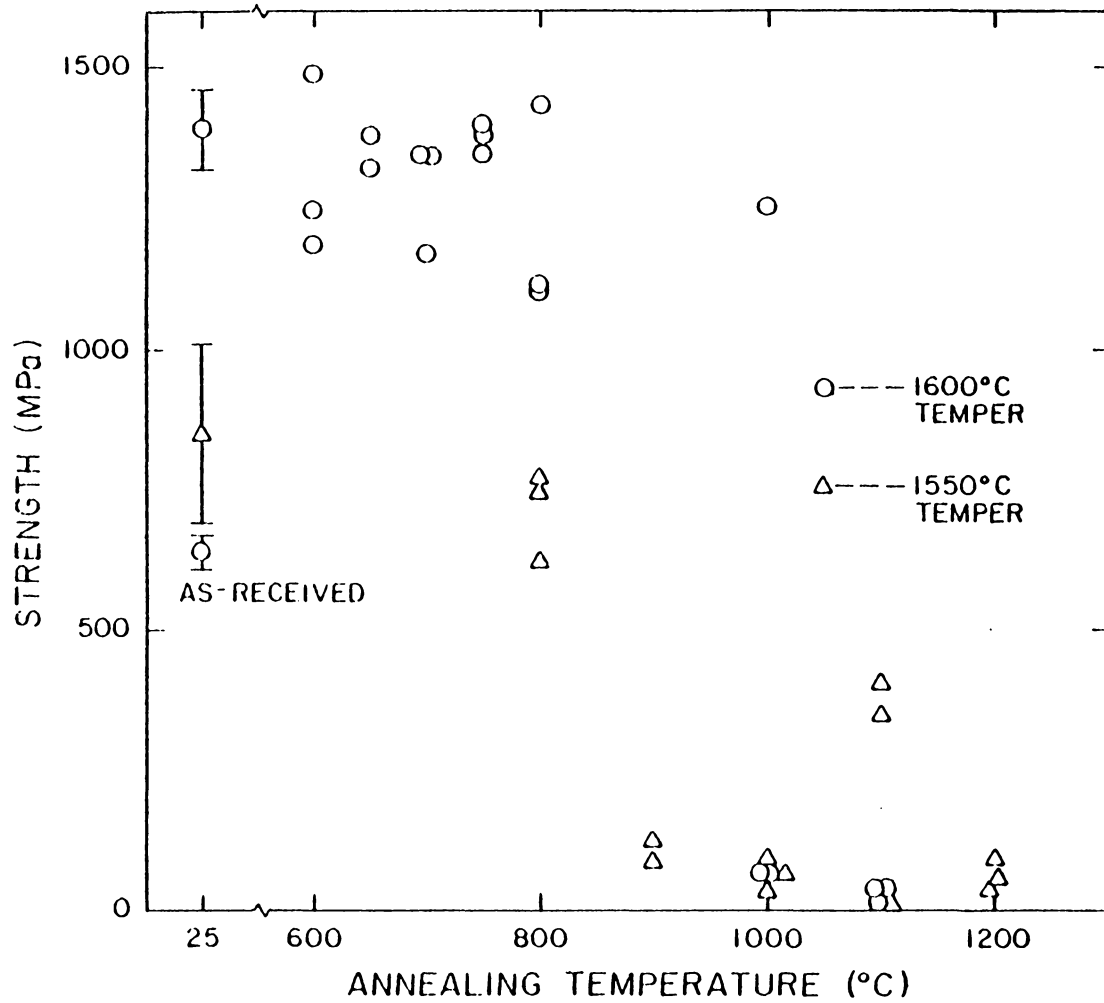


Figure 18. Flexural strength of tempered ALSIMAG 838 alumina after 25 min. anneal, as a function of annealing temperature.

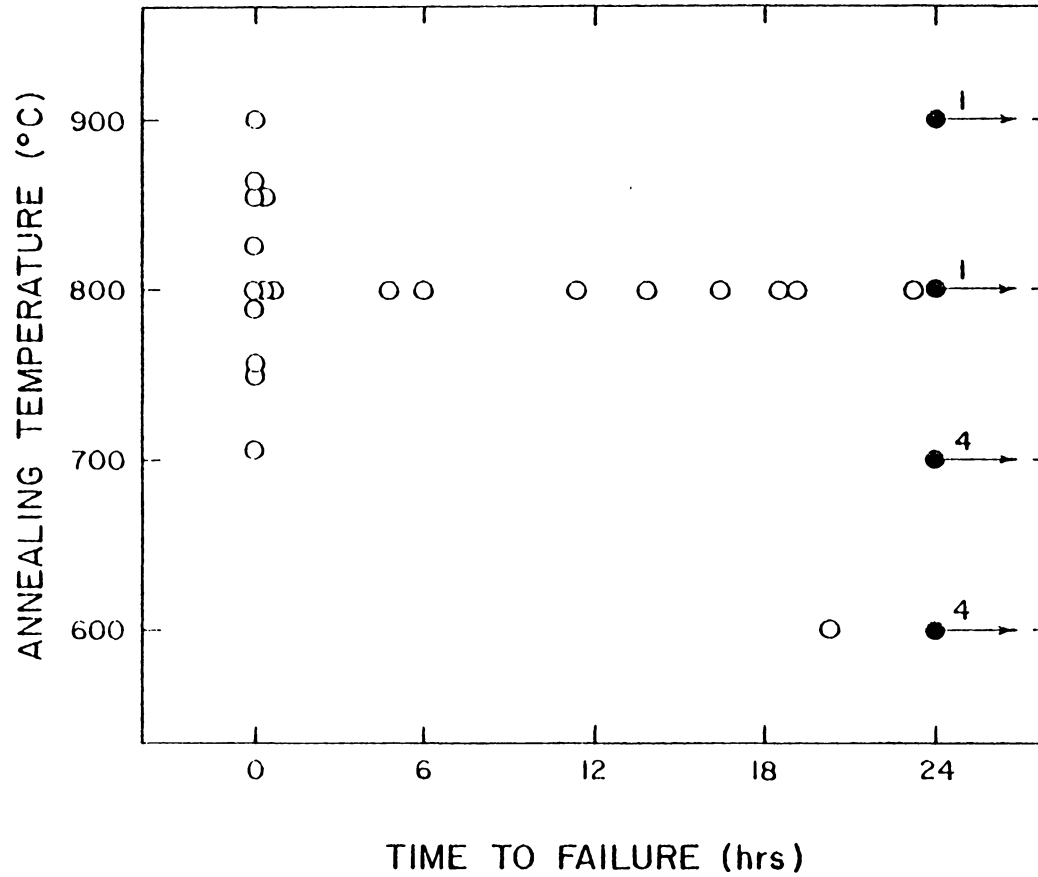


Figure 19. Time-to-failure annealing treatments, under iso-thermal conditions, for the tempered ALSIMAG838 alumina.

heating to 800°C. Most importantly, under isothermal conditions many samples failed at 800°C during the 24 hours.

C. Scanning Electron Fractography (SEF)

Many of the tentative conclusions reached by examining the dilatometric and strength degradation results can be further substantiated with SEF. Fracture behavior such as intergranular and transgranular cracking or viscous deformation of the grain-boundary phase can reveal vital information on the mechanisms of residual stress relaxation.

Figure 20 shows the scanning electron fractograph of a tempered AL-300 alumina that was annealed at 850°C for 25 minutes. Strength result indicates that this specimen has gone through partial stress relaxation, noted by a 300 MPa decrease from the tempered specimen strength. The fracture was done at room temperature. Photo (a) is representative of the fracture behavior at the specimen surface regions, and photo (b) is at the specimen interior. At the specimen surface, transgranular cracking dominated. This may be caused by the compressive stress field that prevented grain separation during annealing. In contrast, intergranular cracking existed at the specimen interior. The existence of glassy intergranular phase is clearly evident. It is possible that due to the compressive stresses, viscous glassy phase is squeezed toward the tensile interior. The geometry of the glassy phase and the absence of cleavage steps at the specimen interior indicate that crack formation occurred at elevated temperatures.

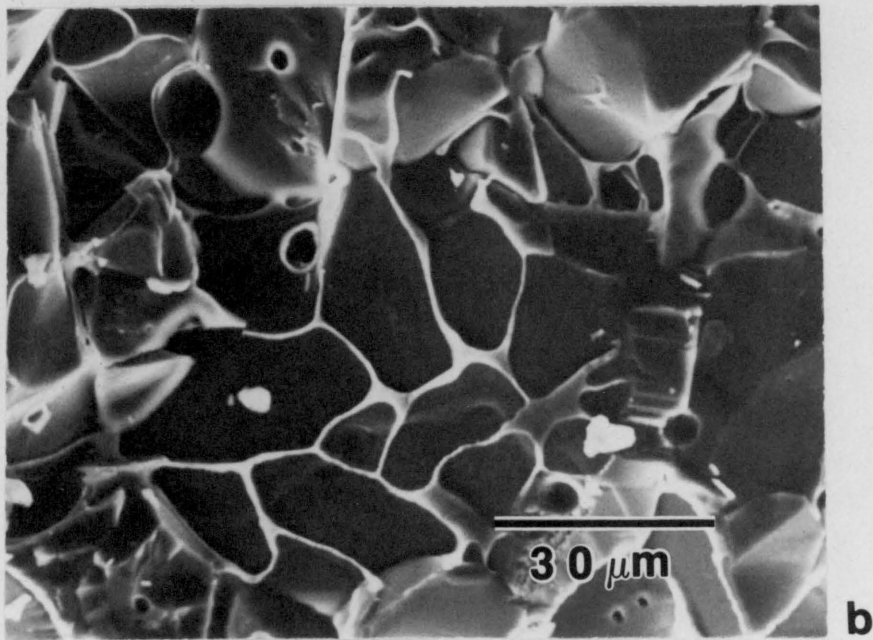
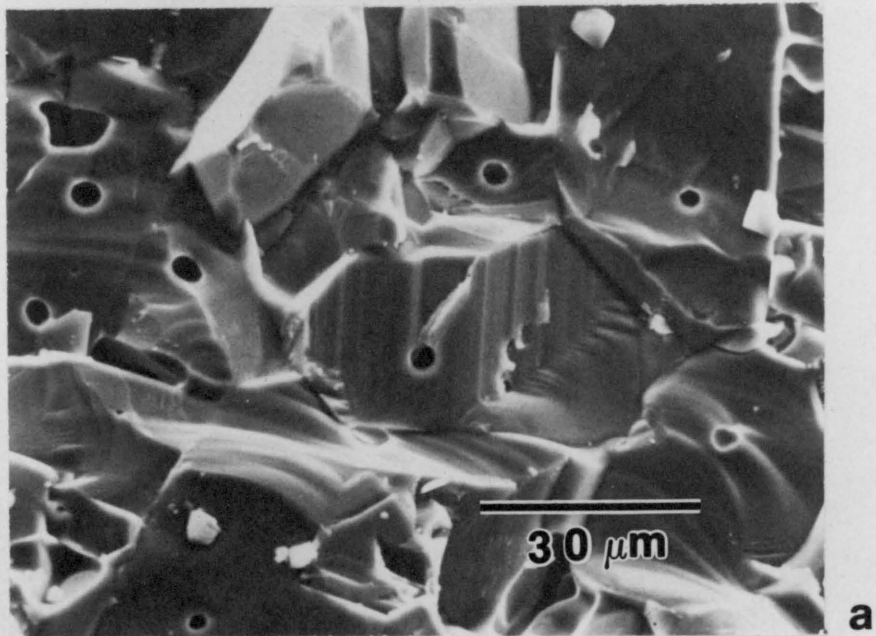


Figure 20. SEM-fractographs of tempered AL-300 alumina fractured at room temperature following annealing treatment at 900°C for 25 min. a) near surface region b) in specimen interior.

Additional fractographs, presented in Figure 21, exhibit further evidence that crack formation occurred at elevated temperatures. Of particular interest is the high magnification photo (b) of the finger-like crack growth. As explained by Fields and Ashby(47), voids or cracks that grow on stressed grain-boundaries will grow in a finger-like fashion advancing ahead of the main body of the void. Raj and Dang(48) also stated that the voids can coalesce and cause grain-boundary de-adhesion. In this photograph, the void may have been residual porosity or triple points that under tensile stress and high temperatures propagated into the grain-boundary and caused de-adhesion. Upon cooling the impression of the finger-like glassy phase remained.

For the ALSIMAG 614 alumina, the retained strength after annealing is much less than the as-received strength. This is due to the higher level of residual stresses driving intergranular cracks into the region originally under compressive stresses. Figure 22(b) clearly shows this behavior. The visible outer ring is the region where transgranular fracture takes place. By measuring the crack radius at different annealing temperatures and comparing it to the specimen radius, one may conclude that the fracture originated at the specimen interior and propagated outward. Results are shown in Figure 23. High magnification fractographs at specimen edge and interior yields similar results as for the AL-300 alumina. However, the viscous glassy phase is not present. Instead, in Figure 24(b), crystallized glass or foreign particles were found in the specimen interior.

As mentioned earlier, ALSIMAG 838 alumina fractured in a cup and

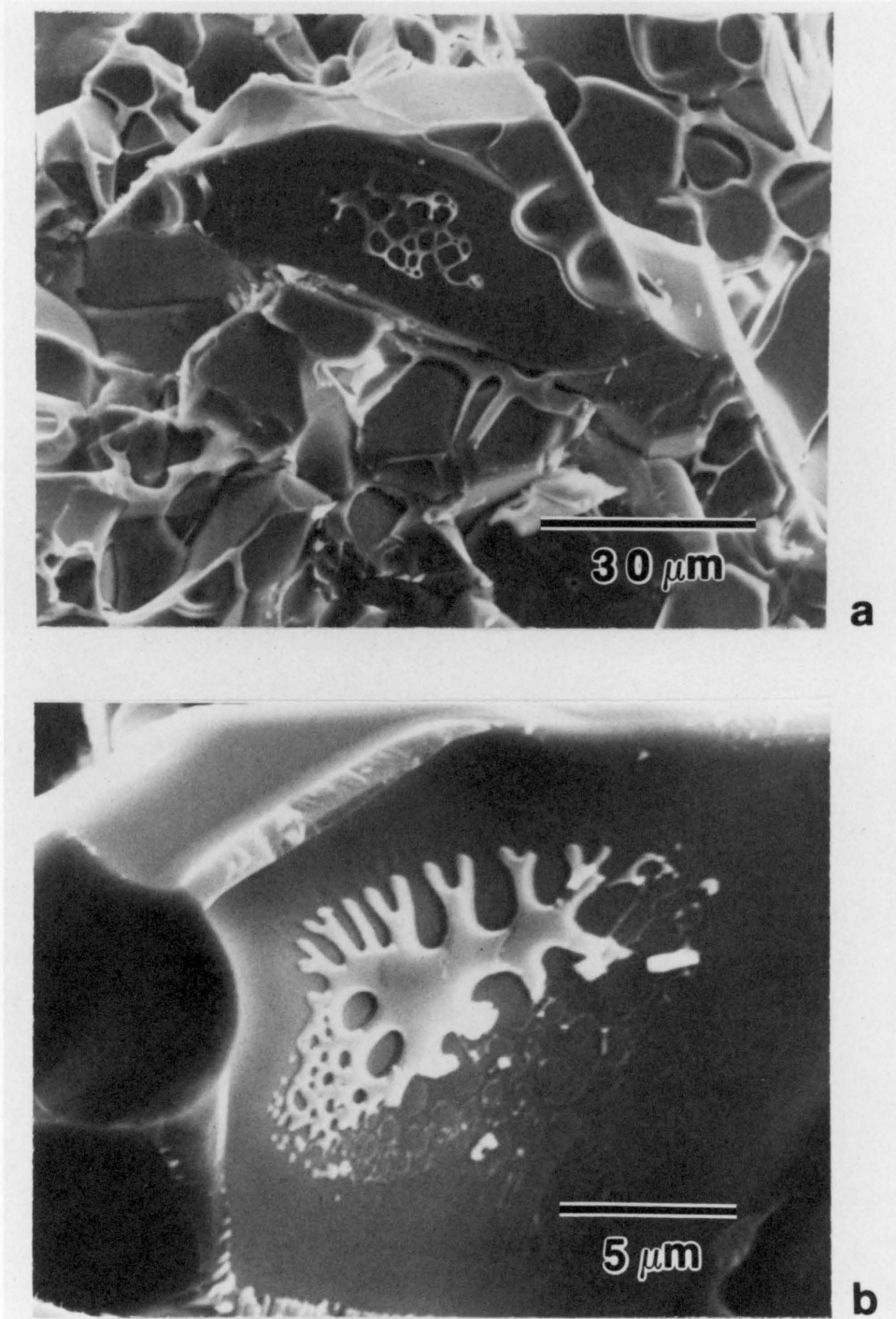


Figure 21. Additional SEM-fractographs of the tempered AL-300 alumina, followed by annealing treatment at 900°C for 25 min. a) existence of glassy intergranular grain-boundary phase, and b) finger-like crack growth indicating rapid grain-boundary de-adhesion at high temperatures.

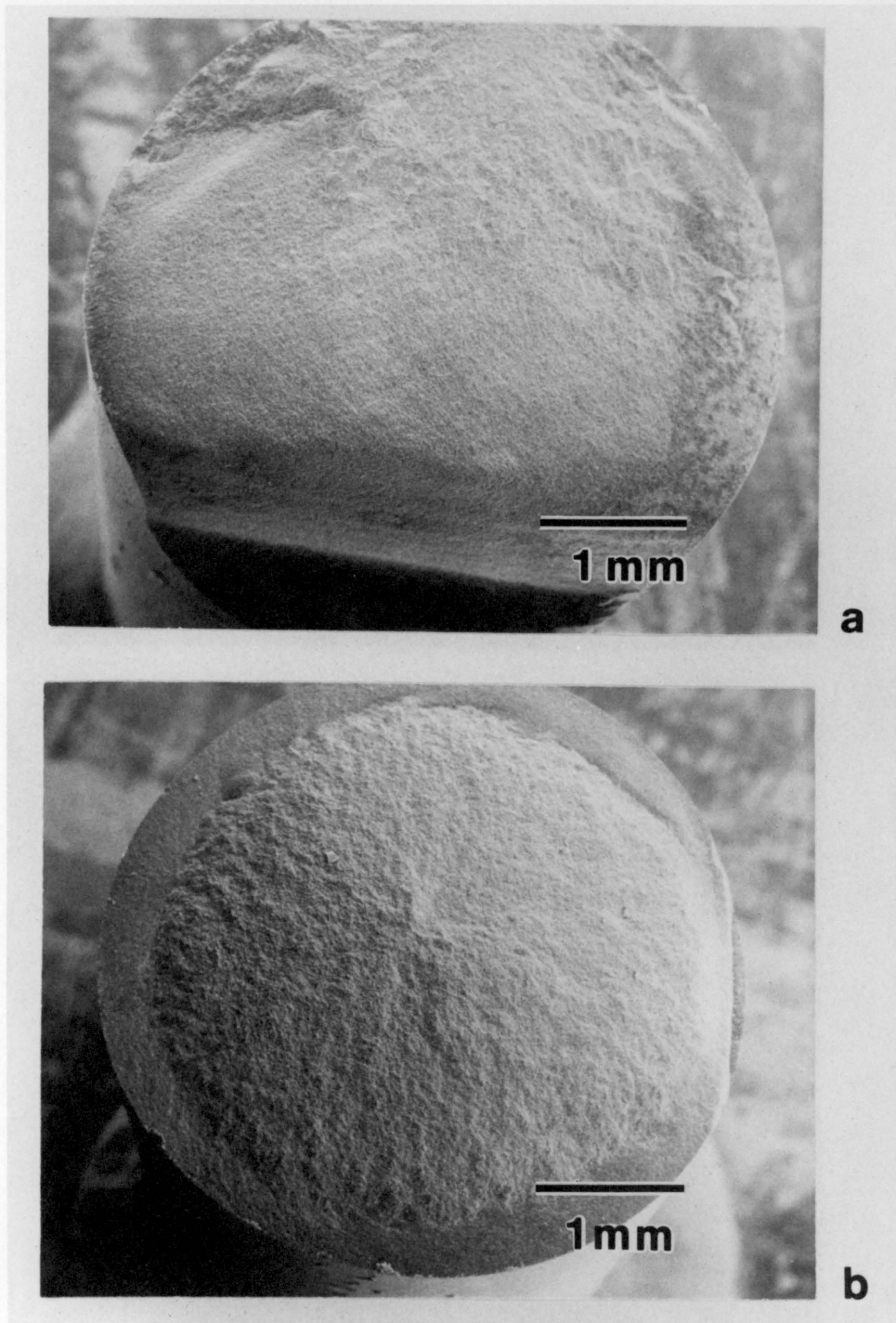


Figure 22. Intergranular crack propagation into original compressive stress field, a) as-received ALSIMAG 614 alumina fractured at room temperature and b) fracture behavior of tempered and then annealed ALSIMAG 614 alumina.

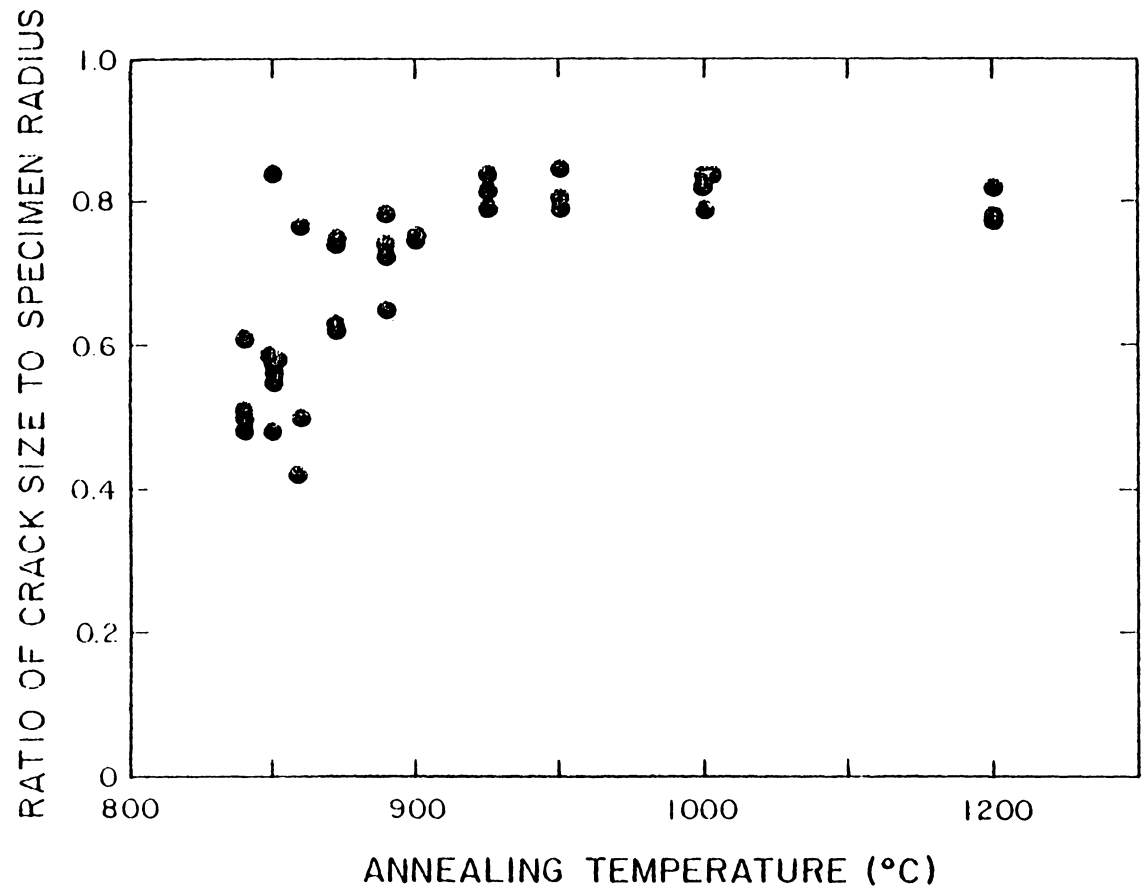


Figure 23. Relative ratio of crack size (radius) to specimen radius.

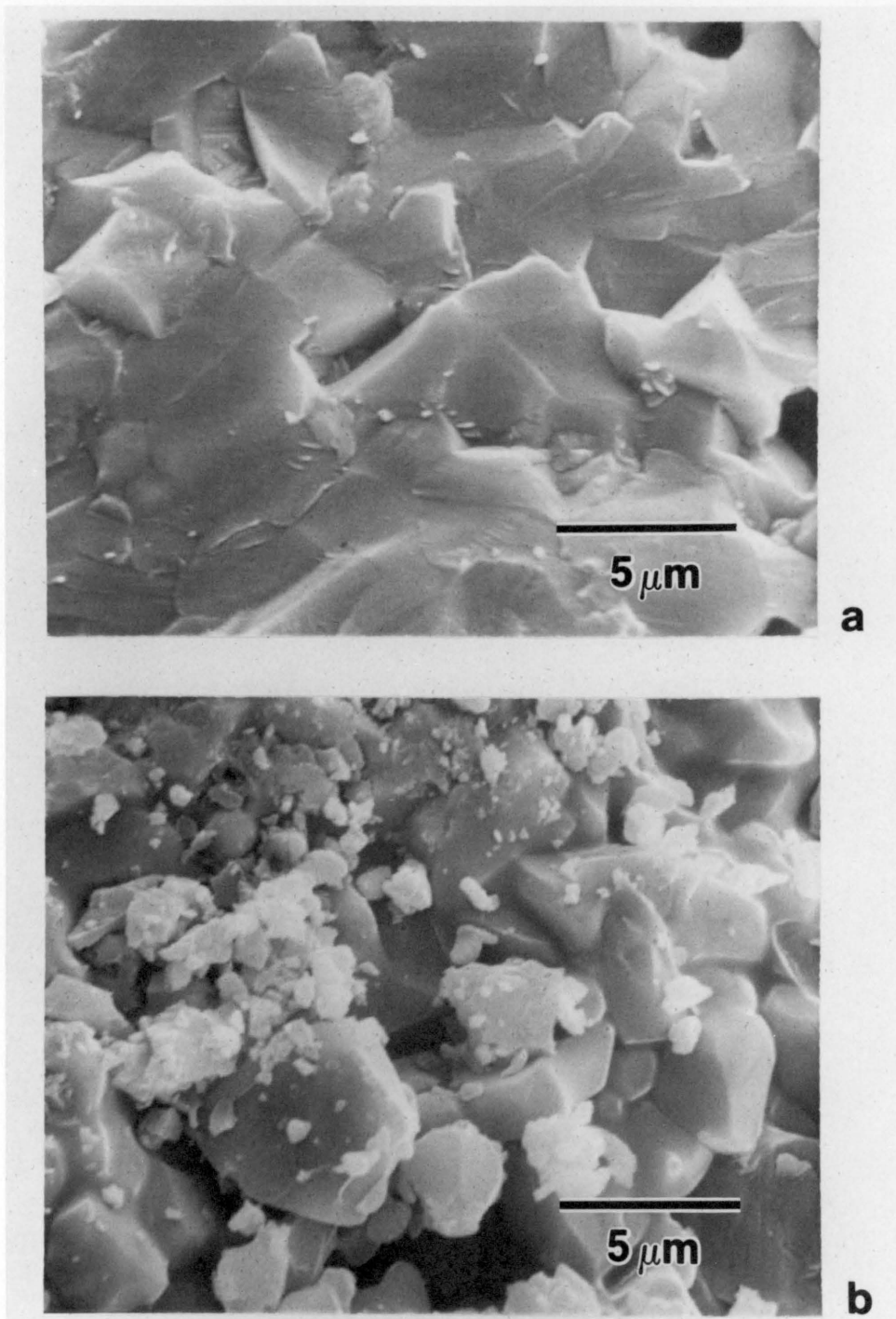


Figure 24. SEM fractographs of the tempered ALSIMAG 614 alumina fractured at room temperature following annealing treatment at 950°C for 25 min. a) near surface region and b) in specimen interior.

cone fashion, shown in Figure 25. Intergranular cracks propagated spontaneously from the specimen's center to the edge. This phenomenon can also be seen from the "pop-in" affect of the dilatometric behavior. No signs of glassy phase was detected. Also as can be seen from Figure 26, intergranular fracture dominated the entire fracture surface.

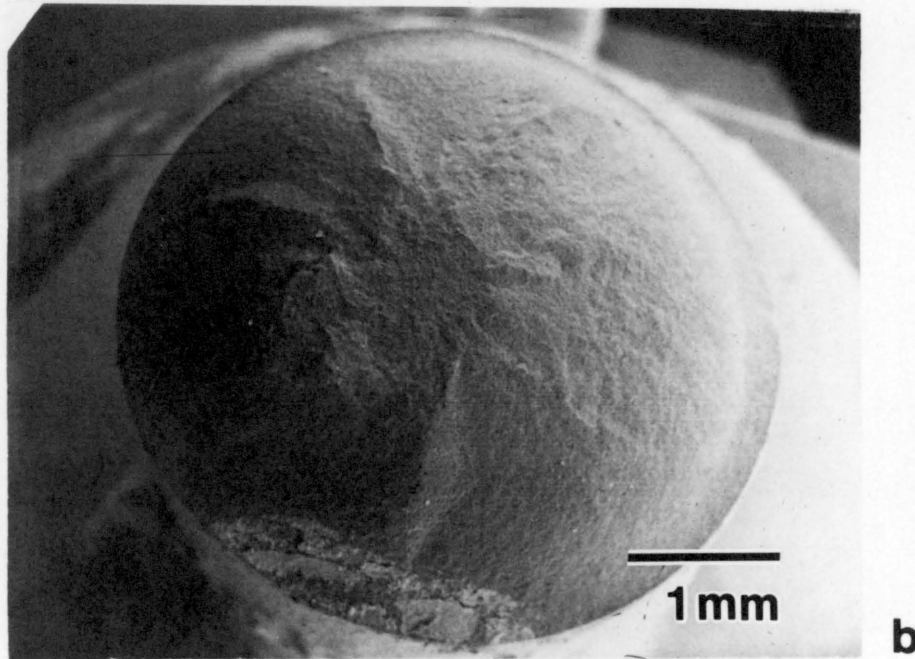
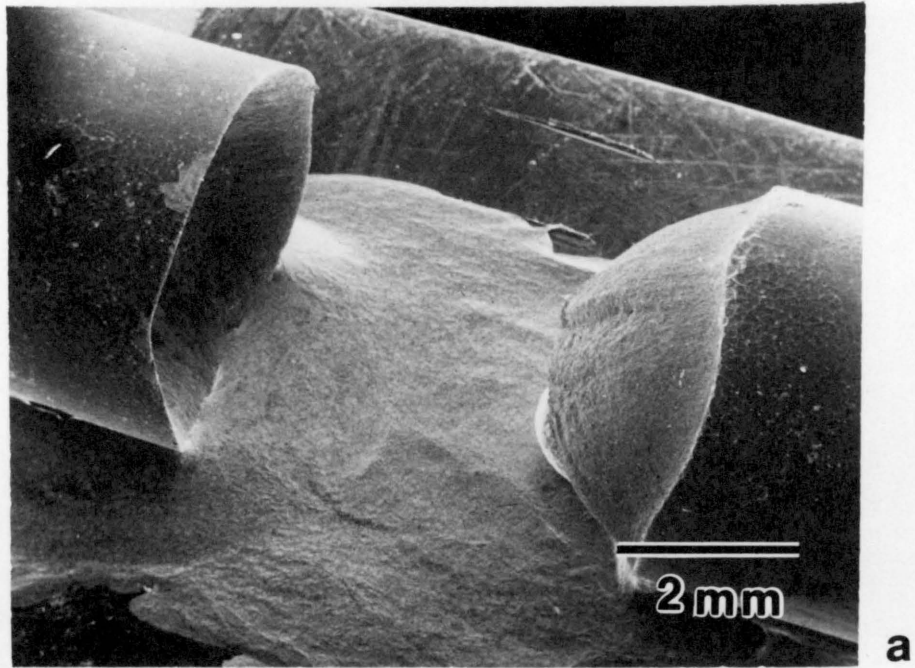
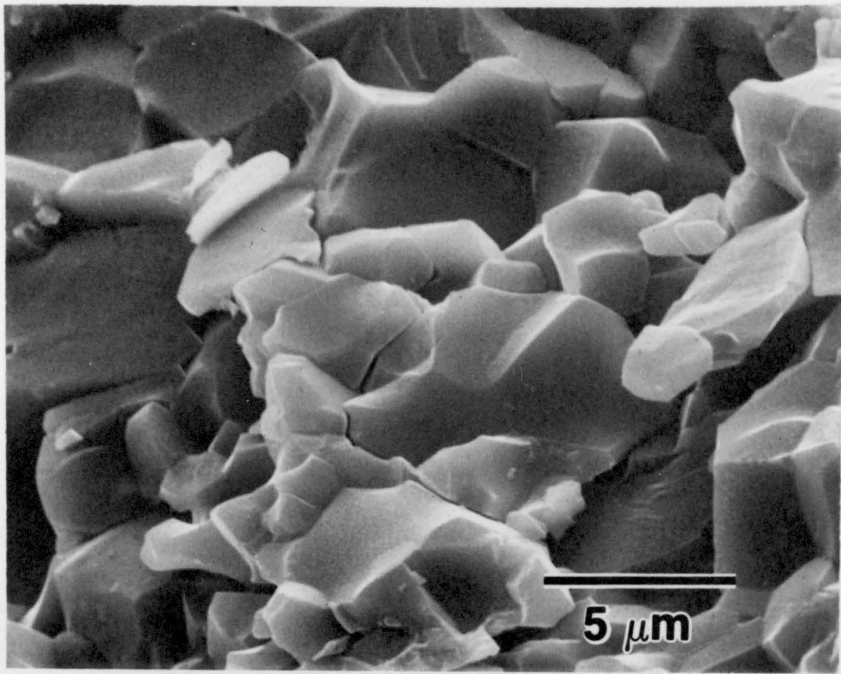
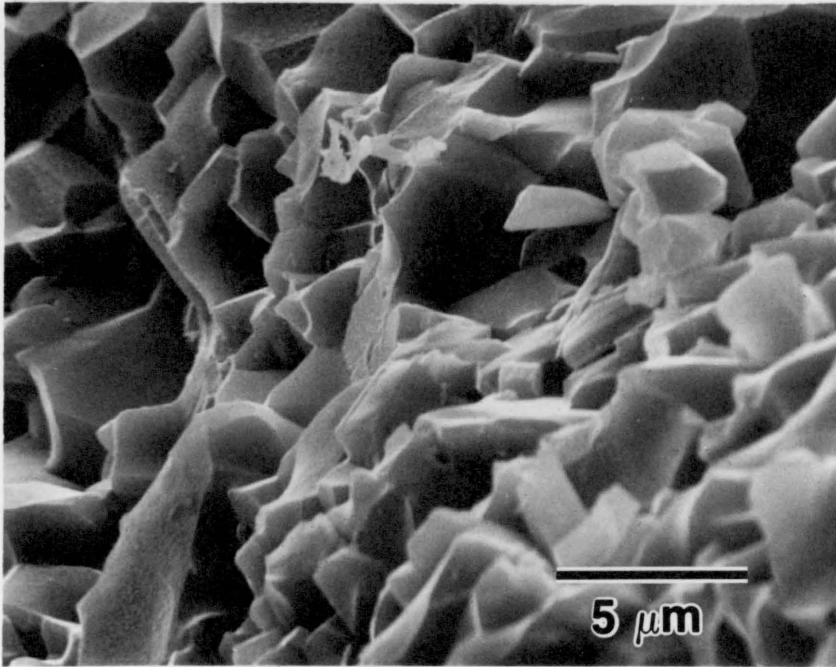


Figure 25. Critical crack propagation, during annealing, in tempered ALSIMAG 838 aluminas resulting in a cup and cone fracture.



a



b

Figure 26. SEM fractographs of the tempered ALSIMAG 838 alumina fractured during annealing treatment, a) near surface region and b) in specimen interior.

D. General Discussion

For all three aluminas studied, the discontinuous behavior in thermal expansion occurred in the same temperature range as for the strength degradation. From these results, one may conclude that the same mechanism was involved for both phenomena.

Stress relaxation by processes such as dislocation motion and diffusional creep exhibits approximately the same rates of creep in tension or compression. Therefore, for tempered specimens with both tensile and compressive residual stress fields, dimensional changes by these processes are expected to be minimal if not non-existent. For the rate of stress relaxation presently observed at this temperature and stress level, dislocation motion and diffusional creep rates are several orders of magnitude too slow to provide a satisfactory explanation(49).

Since the alumina is already in the alpha form, the thermal expansion is not due to some irreversible crystallographic phase transformation. Therefore, in view of the observed strength and fracture behavior, residual stress relaxation by the formation and growth of cracks is the most likely explanation for the present observation.

The results from dilatometric measurements, specimen strength after anneal, and SEF all support that stress relaxation occurred by crack formation and growth. From the dilatometric studies, a permanent increase in length of the specimens upon cooling to room temperature was found. No changes in specimen diameter were detected, so there was a net volume increase. Combined with the strength decreases to below the

as-received strength in most cases, the only explanation can be the formation of cavities or cracks that weakened the specimens.

This is further substantiated with the SEF. At elevated temperatures, the viscosity of the intergranular glassy phase is expected to decrease. Therefore, this would allow de-adhesion of grain-boundaries under tensile stresses. For the tempering method used in this study, tensile residual stresses exist in the interior of the specimen and compressive residual stresses exist at the specimen exterior. Therefore, crack growth occurs only at the specimen interior. This is the reason why intergranular cracks were found at the specimen interior only. At the compressive regions, glassy phase assisted grain-boundary de-adhesion at elevated temperatures were nonexistent. Therefore, transgranular fracture was observed for the specimen near the exterior region. This is the reason for the retained strength after anneal for the AL-300 and ALSIMAG 614 alumina.

Present observations indicate the mechanism responsible for the residual stress relaxation in the aluminas is by crack formation or cavitation. The presence of cracks will lower the elastic modulus(50). Under constant strain conditions, the energy per unit volume is proportional to the elastic modulus. Therefore, a decrease in the elastic modulus will lower the system energy, thus providing the driving force for crack propagation. Accompanying crack growth, the crack opening displacement will increase and lead to increases in specimen dimension. Therefore, the residual stress relaxation in these aluminas is due to creep by crack growth.

A schematic of the crack growth model is shown in Figure 27. Figure 27(a) shows the residual stress distribution after tempering treatment and Figure 27(b) shows the random intergranular crack formation in the tensile stressed region. Because of the coupled nature of residual stresses, stress relaxation in tension will automatically lead to elastic relaxation of the compressive stresses. Also, for the AL-300 alumina, intergranular cracking existed only at the interior; therefore, a cylindrical tube section of the alumina rod did not suffer from grain-boundary de-adhesion, and thus retained partial strength.

A comparison of the dilatometric results of the AL-300 and ALSIMAG 614 aluminas show that crack formation occurred 25°C higher for the AL-300 alumina, and the temperature range for which crack growth occurred was narrower. As noted earlier, crack formation is due to tensile stresses acting on a low viscosity grain-boundary. Therefore, factors such as the magnitude of the tensile stresses, grain-boundary composition and the size of the precursor may have significant effect on the crack formation temperature. For example, the presence of Ca in the AL-300 alumina may lower the viscosity and cause grain-boundary de-adhesion at a lower temperature. Also, the size of the precursor such as cracks or voids can change the stress intensity factor thus influencing the crack growth temperature. It is suggested that the 25°C difference in crack formation temperature presently observed is mainly due to the difference in the magnitude of residual stresses. However, it is not possible to determine the contribution of the other factors.

For the growth of cracks along a grain-boundary phase, it is

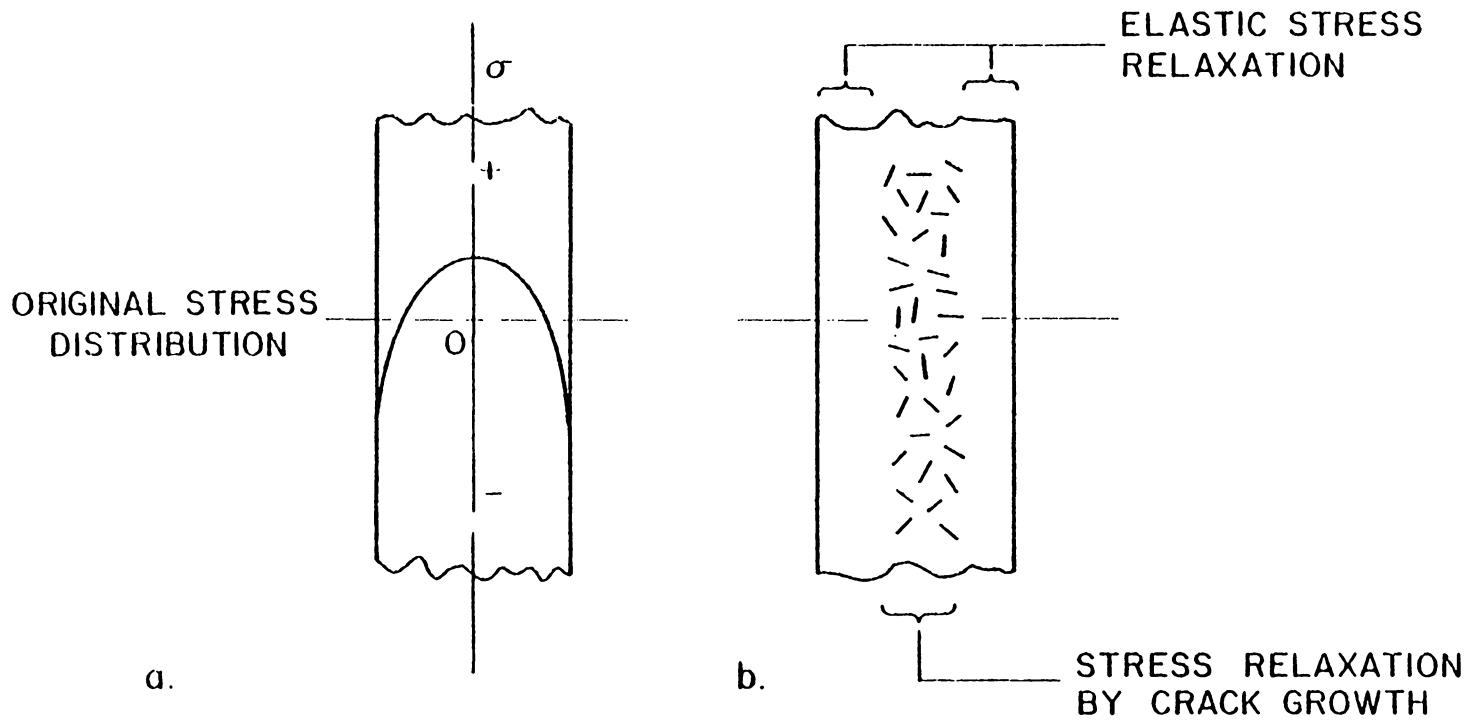


Figure 27. Residual stress relaxation by crack growth (a) original stress distribution and (b) after annealing treatment.

essential to have large amounts of the secondary phase. This is under the assumption that crack growth is by viscous flow or by diffusional processes at the crack-tip. As indicated in Table I, ALSIMAG 614 alumina is expected to contain more glassy phase. However, because the grain size is five times smaller for the ALSIMAG 614 alumina than for the AL-300 alumina, grain-boundary area is expected to increase by a factor of twenty-five. Therefore, even with a large amount of glassy phase, the grain-boundary phase thickness is expected to be much less than the AL-300 alumina. Also, one may have non-uniform distribution of the glassy in the alumina. Under these conditions, crack growth for ALSIMAG 614 alumina should be much more difficult. This may have attributed to the irregular crack growth in the ALSIMAG 614 alumina, while smooth crack growth was observed in AL-300 alumina.

For the AL-300 coarse-grained alumina, residual stress relaxation occurs by viscous deformation of a glassy grain-boundary phase. When the residual stresses are reduced by crack growth, the crack arrests. In contrast, ALSIMAG 838 fine-grained alumina with little intergranular glassy phase exhibited critical crack propagation, indicated by "pop-in" during thermal expansion. This observation can be due to the combined effects of sub-critical crack growth and decrease in the critical stress intensity factor at elevated temperatures(51). Evidence of sub-critical crack growth for the ALSIMAG 838 alumina can be seen in residual stress fatigue results shown in Figure 19. When the tempered specimens were held at 800°C for 24 hours, samples failed at different time intervals. Under isothermal conditions, due to sub-critical growth, cracks can

reach a sufficient size so that for a given magnitude of residual stresses K_{RS} will be equal to K_{IC} and the specimen will fail spontaneously. Critical crack propagation can also occur if the K_{IC} decreases at elevated temperatures until $K_{IC} = K_{RS}$. This latter reason explains the samples that fractured during heating. Both effects can contribute to the data shown in Figure 19.

Obviously, neither crack formation nor critical crack propagation are desirable for residually stressed ceramics in most engineering applications. Therefore, relaxation of residual stresses should not be accomplished by annealing treatments. However, if a component is not used for structural purposes, residual stresses can be annealed if K_{RS} is less than the lowest stress intensity factor, K_0 , required for slow crack propagation. If K_{RS} is greater than K_0 , crack formation cannot be avoided. Since no other residual stress relaxation processes exist, one should minimize the residual stresses during processing. Residual stresses should be kept below the threshold for slow crack growth. If a structural ceramic component is tempered for load-carrying purposes, it should not be used at temperatures at which crack formation would occur.

An alternative approach would be to suppress the crack formation. Several methods can be used to suppress crack formation. First, the amount of viscous glassy grain-boundary phase should be kept to a minimum. This can be achieved by using highest purity alumina available and to decrease the grain size. Furthermore, since crack formation requires precursors in the form of pores at grain boundaries or triple points, these should be kept as small as possible if not eliminated

altogether. Also, one may make chemical modification of the glassy phase to increase the viscosity at elevated temperatures and impede crack growth.

IV. CONCLUSIONS

The conclusions drawn from the results of this study are:

1. Residual stress relaxation in polycrystalline aluminum oxide can be achieved at elevated temperatures by crack growth in regions under tensile stresses.

2. At elevated temperatures, the intergranular glassy phase acts as a viscous adhesive layer causing grain-boundary de-adhesion under tensile stresses.

3. Existence of glassy grain-boundary phase, residual porosity, large grain size and high magnitude of residual stresses can contribute to the formation and propagation of intergranular cracks.

4. Residually stressed fine-grained polycrystalline aluminum oxide, with little or no glassy phase, can undergo fatigue by sub-critical crack propagation under isothermal conditions and change to critical crack propagation when $K_{RS} = K_{IC}$.

5. Reduction of high levels of residual stresses in polycrystalline aluminum oxide should not be done by annealing treatments, because crack nucleation and growth will substantially reduce the load-carrying ability.

For aluminas with a high level of residual stresses one may delay or avoid the nucleation and propagation of intergranular cracks depending on the material application. First, the residual stresses should be kept lower than that required for subcritical crack growth. Second, for a given material, impurities, porosity, inclusions, ect. should be minimized. Also, the grain size may be decreased in order to disperse the intergranular glassy phase.

REFERENCES

- (1) National Aeronautics and Space Administration, Nondestructive Testing - A Survey, United States Government Printing Office, NASA SP-5113, (1973).
- (2) K. Masubuchi, Analysis of Welded Structures, Pergamon Press, (1980).
- (3) W.D. Kingery, Introduction to Ceramics, Wiley, New York, (1960).
- (4) A.G. Cockbain, Proceeding of the British Ceramic Society, vol.25, 253, (1975).
- (5) The Committee on Ceramic Processing, Ceramic Processing, National Academy of Sciences, Washington D.C., (1968).
- (6) F. Kools, Chapter 3, Science of Ceramics, vol.7, Societie Francaise de Ceramique, (1973).
- (7) A.G. Evans, Abrasive Wear in Ceramics: An Assessment, NBS Special publication 562, (1979).
- (8) B.R. Lawn and T.R. Wilshaw, Journal of Material Science, vol. 10, 1049, (1975).
- (9) R.H. Insley and V.J. Barczak, Journal of the American Ceramic Society, vol. 47, 1-4, (1964).
- (10) W.D. Kingery, Ceramic Fabrication Processes, Massachusetts Institute of Technology, (1968).
- (11) A.K. Varshneya and R.J. Petti, Journal of the American Ceramic Society, vol. 59, 42, (1976).
- (12) M.P. Borom and R.A. Giddings, Ceramic Bulletin, vol. 55, 1046, (1976).
- (13) R.W. Rice, Material Engineering, vol. 30, (1971).
- (14) H.P. Kirchner, R.M. Gruver and R.E. Walker, American Ceramic Society Bulletin, vol. 9, 47, 798-802, (1968).
- (15) D.R. Platts, et al., Journal of the American Ceramic Society, 53, vol. 5, 281, (1970).
- (16) M.A. Hussain and S.L. Pu, Journal of Applied Physics, vol. 21, 853, (1950).
- (17) R.C. Pohanka, R.W. Rice and B.E. Walker, Journal of the American

- Ceramic Society, vol. 59, 71, (1976).
- (18) K.M. Merz, W.R. Brown and H.P. Kirchner, *Journal of the American Ceramic Society*, vol. 45, 531, (1962).
 - (19) G.Y. Onoda and L.L. Hench, Ceramic Processing Before Firing, Wiley, (1978).
 - (20) J. Weertman, *Transaction of the Metal Society A.I.M.E.*, vol. 227, 1475, (1965).
 - (21) F.R.N. Nabarro, *Conference on Strength of Solids*, 72, Physical Society, London, (1948).
 - (22) C. Herring, *Journal of Applied Physics*, vol. 21, 437, (1950).
 - (23) R.L. Coble, *Journal of Applied Physics*, vol. 34, 1679, (1963).
 - (24) D.A. Krohn, P.A. Urick, D.P.H. Hasselman and T.G. Langdon, *Journal of Applied Physics*, vol. 45, 3729, (1974).
 - (25) R.M. Gruver and W.R. Buessem, *American Ceramic Society Bulletin*, 9, vol. 47, 749-751, (1971).
 - (26) H.P. Kirchner and R.M. Gruver, *Material Science and Engineering*, vol 13, 63-69, (1974).
 - (27) H.P. Kirchner, Strengthening of Ceramics, Marcel Dekker, New York, (1979).
 - (28) D.P.H. Hasselman, *Journal of the American Ceramic Society*, vol. 42, 417, (1969).
 - (29) A. Venkateswaran and D.P.H. Hasselman, *Journal of Material Science*, vol. 16, 1627-1632, (1981).
 - (30) J.F. Lynch, C.G. Ruderer, and W.H. Duckworth, editors, Engineering Properties of Selected Ceramic Materials, American Ceramic Society, Columbus OH, (1966).
 - (31) Mechanical and Electrical Properties of ALSIMAG Ceramics, Company Data, American Lava Corporation, Chattanooga TN, USA.
 - (32) S.D. Stookey, High Strength Materials, Wiley, New York, 669-681, (1964).
 - (33) D.A. Krohn and A.R. Cooper, *Journal of the American Ceramic Society*, vol. 51, 2, 98-102, (1968).
 - (34) S.S. Kistler, *Journal of the American Ceramic Society*, vol. 45, 2,

- 59-68, (1962).
- (35) A.J. Burggraaf, *Physics and Chemistry of Glasses*, vol. 7, 5, 169-172, (1966).
 - (36) R.M. Gruver and H.P. Kirchner, *Journal of the American Ceramic Society*, vol. 51, 232-233, (1967).
 - (37) H.P. Kirchner, R.E. Walker and D.R. Plotts, *Journal of Applied Physics*, vol. 42, 10, 3685, (1971).
 - (38) W.R. Buessem and R.M. Gruver, *Journal of the American Ceramic Society*, vol. 55, 101, (1972).
 - (39) B.K. Sarkar and T.G. Glimm, *Transactions of the British Ceramic Society*, vol. 69, 5, 199-203, (1970).
 - (40) R.K. Kirby, *Mechanical and Thermal Properties of Ceramics*, Proceedings of a symposium, 41-61, (1968).
 - (41) P.K. Foster and I.R. Hughes, *Journal of the American Ceramic Society*, vol. 49, 515, (1966).
 - (42) W.D. Kingery, *Journal of the American Ceramic Society*, vol. 38, 3, (1955).
 - (43) E.A. Bush and F.A. Hummel, *Journal of the American Ceramic Society*, vol. 42, 388, (1959).
 - (44) W.D. Kingery, *Journal of the American Ceramic Society*, vol. 40, 351, (1957).
 - (45) O. Hunter and W.E. Brownell, *Journal of the American Ceramic Society*, vol. 50, 19, (1967).
 - (46) J.F. Lynch, C.G. Ruderer and W.H. Duckworth, Engineering Properties of Selected Ceramic Materials, The American Ceramic Society Incorporated, 1966.
 - (47) R.J. Fields and M.F. Ashby, *Philosophical Magazine*, vol. 33, no. 1, pp. 33-48, 1976.
 - (48) R. Raj and C.H. Dang, *Philosophical Magazine*, vol. 32, no. 5, pp. 909-922, Nov. 1975.
 - (49) T.G. Langdon, *Metals Forum*, vol. 1, no. 2, p. 59, 1978.
 - (50) W.R. Delamater, G. Herrmann and D.M. Barnett, *Journal of Applied Mechanics*, p. 74, March 1975.

- (51) A.G. Evans, M. Linzer and L.R. Russell, Material Science and Engineering, vol. 15, p. 253, 1974.
- (52) S. Timoshenko and J.N. Goodier, Theory of Elasticity, McGraw-Hill Book Company, Inc., third edition, p. 445, 1951.
- (53) H.S. Carslaw and J.C. Jaeger, Conduction of Heat in Solids, Oxford University Press, second edition, p. 201, 1959.

APPENDIX

Thermal stress calculation for alumina specimens subjected to 10°C/min heating rate.

a) Thermal stress for long circular cylinders in the axial direction(50)

$$\sigma_z = \frac{\alpha E}{1-\nu} \left(\frac{2}{b^2} \int_0^b T r \, dr - T \right) \quad (1)$$

b) Radial flow of heat in an infinite cylinder with variable surface temperature(51)

$$T = K \left(t - \frac{b^2 - r^2}{4k} \right) = Kt - \frac{Kb^2}{4k} + \frac{4r^2}{4k} \quad (2)$$

Substitute equation (2) into equation (1).

$$\sigma_z = \frac{\alpha E}{1-\nu} \left[\frac{2}{b^2} \int_0^b \left(Kt - \frac{Kb^2}{4k} + \frac{Kr^2}{4k} \right) r \, dr - Kt + \frac{Kb^2}{4k} - \frac{Kr^2}{4k} \right]$$

$$\sigma_z = \frac{\alpha E}{1-\nu} \left[\frac{2Kb^2}{b^2} \left(\frac{t}{2} - \frac{b^2}{16k} \right) - Kt + \frac{Kb^2}{4k} - \frac{Kr^2}{4k} \right]$$

$$\sigma_z = \frac{\alpha EK}{(1-\nu)4k} \left[\frac{b^2}{2} - r^2 \right]$$

$$\alpha \text{ (thermal expansion)} = 7 \times 10^{-6}$$

$$E \text{ (Young's Modulus)} = 344 \times 10^9 \text{ N/m}^2$$

$$K \text{ (heating rate)} = 0.167 \text{ }^\circ\text{C/sec}$$

$$\nu \text{ (Poisson's ratio)} = 0.22$$

$$k \text{ (thermal diffusivity)} = 0.01 \text{ cm}^2/\text{sec}$$

$$b \text{ (specimen radius)} = 0.252 \text{ cm}$$

$$\sigma_z = 136.4 \text{ kPa} \approx 20 \text{ psi}$$

**The vita has been removed from
the scanned document**

DEFORMATION AND FRACTURE BEHAVIOR DURING
ANNEALING OF RESIDUALLY STRESSED POLYCRYSTALLINE

ALUMINUM OXIDE

by

Yenho Kuo Tree

ABSTRACT

Three types of polycrystalline aluminum oxide, with varying amounts of impurities, were tempered and then annealed to study the behavior of residual stress relaxation. Results from microprobe analysis, thermal expansion analysis, annealed strength measurements, and scanning electron fractography clearly indicate stress relaxation at annealing temperatures occurred by elastic creep through crack nucleation and growth in regions under tensile stresses. From the scanning electron fractographs, it was found that intergranular glassy phase played an important role in the crack formation and propagation. At elevated temperature, viscous intergranular glassy phase behaved as an adhesive layer and when under tensile stresses caused de-adhesion of grain-boundaries or the formation of cracks. Fine-grained aluminas, with little or no glassy phase, exhibited both sub-critical and critical crack propagation. Since cracks decrease the load-carrying ability of the aluminas, it was concluded that by minimizing the glassy phase, porosity, grain size and residual stresses one can suppress crack formation.